Article

4-Benzoylamino-3-hydroxybutyric acid – historically first “anomalous racemate”: reinvestigation

Alexander A Bredikhin, Zemfira A Bredikhina, Dmitry V Zakharychev, Aida I Samigullina, and Aidar T. Gubaidullin

Cryst. Growth Des., **Just Accepted Manuscript** • DOI: 10.1021/cg5017615 • Publication Date (Web): 12 Feb 2015

Cover Page

4-Benzoylamino-3-hydroxybutyric acid – historically first "anomalous racemate": reinvestigation

Alexander A. Bredikhin*, Zemfira A. Bredikhina, Dmitry V. Zakharychev, Aida I. Samigullina, and Aidar T. Gubaidullin

A.E. Arbuzov Institute of Organic and Physical Chemistry of Kazan Scientific Center of Russian Academy of Sciences, Arbuzov St., 8, Kazan 420088, Russian Federation

The chiral 4-benzoylamino-3-hydroxybutyric acid (**1**) was recognized in 1930 as the first example of "anomalous racemates" (correct to say – anomalous conglomerates), i.e. specific addition compounds formed by different enantiomers in unequal ratio. Through the comparative (racemic against homochiral samples) investigation using IR spectrometry, single crystal X-ray diffraction, PXRD analysis, and solubility studies, we have found that this substance forms a normal racemic compound in the solid state, and thus must be excluded from the very short list of anomalous conglomerates. At the same time *homo*-**1** is dissolved in 25 times better than *rac*-**1**, and this feature belongs to another interesting and rare type, namely "anticonglomerates". We discuss some of the reasons for this behavior.

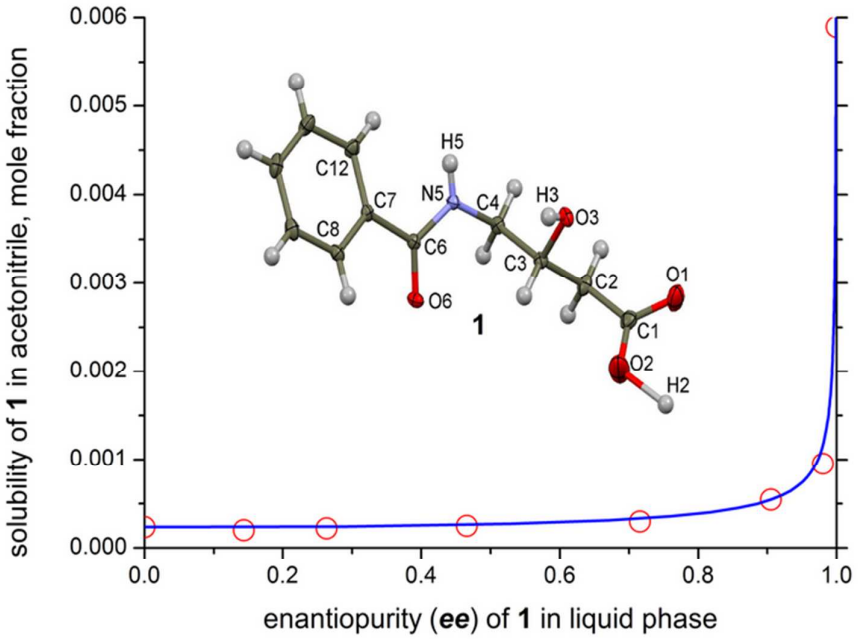

* Corresponding author: Phone/fax: +7 843 2727393/ +7 843 2731872. E-mail: baa@iopc.ru.

4-Benzoylamino-3-hydroxybutyric acid, historically first "anomalous racemate": reinvestigation

Alexander A. Bredikhin,* Zemfira A. Bredikhina, Dmitry V. Zakharychev, Aida I. Samigullina, Aidar T. Gubaidullin

A.E. Arbuzov Institute of Organic and Physical Chemistry of Kazan Scientific Center of Russian Academy of Sciences, Arbuzov St., 8, Kazan 420088, Russian Federation

ABSTRACT

Chiral 4-benzoylamino-3-hydroxybutyric acid (**1**) was recognized in 1930 as the first example of "anomalous racemates" (correct to say – anomalous conglomerates), i.e. specific addition compounds formed by different enantiomers in unequal ratio. Through the comparative (racemic against homochiral samples) inspection of the IR spectra, single crystal X-ray diffraction, PXRD analysis, and solubility data we have found that this substance forms normal racemic compound in the solid state, and must be excluded from the very short list of anomalous conglomerates. At the same time *homo*-**1** is dissolved in 25 times better than *rac*-**1**, and this feature belongs to another interesting and rare type, namely "anticonglomerates". Some of the reasons for this behavior are discussed.

INTRODUCTION

Chiral 4-benzoylamino-3-hydroxybutyric acid (**1**) is structurally resemblant to the important neurotransmitter γ-amino-n-butyric acid (GABA) and may serve as a precursor in the synthesis of carnitine, an essential cofactor of fatty acid metabolism (Scheme 1). In this latter capacity the amino acid **1** attracts the attention of chemists for over a century.

Scheme 1. Benzoylaminohydroxybutyric acid **1** and related biologically important compounds

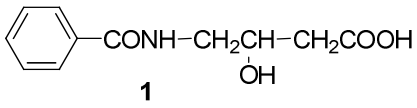

1

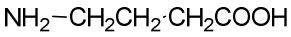

GABA

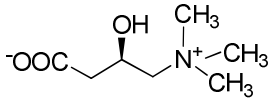

Carnitine

In 1930, when attempting to obtain enantiopure acid **1** by crystallisation of the samples of intermediate enantiomeric composition, Bergman and Lissitzin found that the enantiomer ratio in the thus formed crystalline precipitate is close to an integer ratio of 2:1.[1] Based on this fact, the authors concluded that the molecular addition compound of suitable composition was formed in the solid phase during crystallization. To emphasize the difference from typical for chiral substances "racemic compound", i.e., addition compound with a ratio of enantiomers of 1:1, for the so detected new crystal type Bergman and Lissitzin coined the term "anomalous racemate".[1] Under this name the phenomenon of crystallization of chiral substances, which form a regular (not caused by disorder of the crystal) addition compounds with unequal ratios of enantiomers, have been discussed in the well-known monograph by Jacques et al.[2]

Amino acid **1** opens the list, given in the monograph,[2] which consists of only 9 compounds. Subsequently, on the one hand, a number of novel compounds have been attributed to this class. On the other hand, new studies were published in which the phase behavior of compounds, previously ranked as "anomalous racemates", received other interpretation. Analysis of the current state of the problem is presented in our review.[3] Virtually, if one considers only configurationally stable chiral compounds, the existence in the solid phase of the addition compounds with unequal ratios of enantiomers is reliably proven only for compounds **2**, **3** and **4** (Scheme 2).[4-6]

Scheme 2. Proven examples of “anomalous racemates”

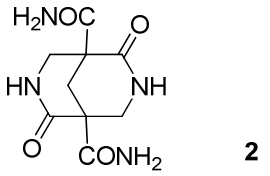

2

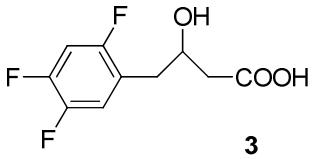

3

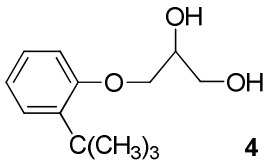

4

Before continuing the discussion, it seems appropriate to make a point about the terminology used. The existence in the unit cell of the crystal of unequal amounts of enantiomers excludes the presence of the symmetry elements of the second kind. Consequently, such compounds should crystallize into one of the 65 Sohncke space groups. This condition inevitably leads to formation of two enantiomorphic crystal modifications during the equilibrium crystallization of the chiral compound from its racemate.[7-9] A mixture of two non-identical crystalline phases should be considered as a conglomerate.

We offered to classify the all possible for a chiral substance conglomerates according the enantiomeric excess of the asymmetric unit of the unit cell, $ee_{\text{as.u.}}$.[9] Following this classification, the name of *normal* or *common conglomerates* refers to those ones, in which each single crystal is formed by a single enantiomer; of course, $ee_{\text{as.u}} = 1$ for these cases. Such conglomerates are most known; they are formed during crystallization of racemic chiral substances prone to spontaneous resolution. For the second group of conglomerates $ee_{\text{as.u}} = 0$. This means that the asymmetric unit is composed of equal amounts of opposite enantiomers, and the single crystal in whole has a racemic composition. In this case, the corresponding sites of the enantiomorphous crystal are occupied with the opposite enantiomers. For the first time this type of conglomerates was noticed by Bishop and Scudder,[10] they proposed the name of *false conglomerates* for them. In more detail this

phenomenon (under the name of *kryptoracemates*) was described by Fábián and Brock; kryptoracemates were found to account for 0.1% of all organic structures containing either a racemic compound, a *meso* molecule, or some other achiral molecule.[11]

The third and the last group of conglomerates comprise those, in which the asymmetric unit is formed by molecules of various enantiomers, but in unequal amounts. Thus the enantiomeric purity of the asymmetric unit may be in principle any rational number between $1 > ee_{as.u} > 0$. For obvious reasons, $Z' \geq 3$ for this class of crystals. We proposed to call this class of addition compounds with unequal ratio of enantiomers as *anomalous conglomerates,* instead of an inadequate name of anomalous racemates.[9]

Apparently anomalous conglomerates are the most rare crystal types for a chiral substance, and are represented in nature by exceptional examples. Therefore, each member of this class deserves close investigation. Meanwhile, the compound that opens the list, i.e. 4-benzoylamino-3-hydroxy-butyric acid **1**, remains in fact unexplored nor in terms of crystallography, nor in terms of phase behavior. In this paper we have attempted to fill this gap, at least partially.

EXPERIMENTAL SECTION

Instrumentation. The NMR spectra were recorded on a Bruker Avance-400 spectrometer (399.9 MHz for ^{1}H and 100.5 MHz for ^{13}C) in DMSO-D_6 or $CDCl_3$ with TMS or the signals of the solvent as the internal standard. The IR spectra of the polycrystalline samples of *rac*- and *scal*-compounds in KBr pellets were recorded on a Bruker Tensor 27 spectrometer. Optical rotations were measured on a Perkin-Elmer model 341 polarimeter (concentration *c* is given as g/100 mL). Melting points for general purposes were determined using a Boëtius apparatus and are uncorrected. HPLC analyses were performed on a Shimadzu LC-20AD system controller, using UV detector.

Substances. Racemic and enantiopure 4-benzoylamino-3-hydroxybutyric acid, *rac*-**1** and (*R*)-**1**, were prepared from *rac*- and (*S*)-epichlorohydrin as shown in Scheme 3. A detailed description of the experiment and the physicochemical characteristics of the intermediates are given in the Electronic Supplement.

(*R*)-4-Benzoylamino-3-hydroxybutyric acid, (*R*)-1. Mp 114–116 °C; $[\alpha]_D^{20}$ = -11.1 (c 1.7, H_2O). {lit.[12]: mp 112-113 °C, $[\alpha]_D^{20}$ = -11.2 (c 1.4, H_2O)}; $[\alpha]_D^{20}$ = -22.5 (*c* 1.0, 0.5 N aq. NaOH). {lit.[1]: $[\alpha]_D^{20}$ = -22 (in 0.5 N aq. NaOH)}; 98 % ee [chiral HPLC analysis of the methyl ether of (*R*)-**1**, which was obtained by the reaction between (*R*)-**1** and CH_2N_2; Daicel Chiralcel OJ (0.46 x 25 cm) column; eluent: hexane/isopropanol = 9:1; flow rate: 1.0 mL/min; UV detector 254 nm (t_R = 17.4 min (major), t_R = 23.4 min (minor)]. ^{1}H NMR (DMSO-D_6): δ = 2.24 (dd, *J* = 8.6, 15.3 Hz; 1H, C*H*HC=O), 2.45 (dd, *J* = 4.2, 15.3 Hz; 1H, CH*H*C=O), 3.30 (m, 2H, CH_2N), 4.07 (m, 1H, CH), 4.98 (br.s, 1H, OH), 7.44-7.54 (m, 3H, Ph), 7.85-7.87 (m, 2H, Ph), 8.42 (t, *J* = 5.7 Hz; 1H, NH), 12.04 (br.s., 1H, COOH). ^{13}C NMR (DMSO-D_6): δ = 41.6 (C-2), 46.4 (C-4), 67.4 (C-3), 128.1 ($C^{2,6}{}_{Ar}$), 129.1 ($C^{3,5}{}_{Ar}$), 132.0 ($C^{4}{}_{Ar}$), 135.4 ($C^{1}{}_{Ar}$), 167.4 (C=O), 173.7 (C-1).

***rac*-4-Benzoylamino-3-hydroxybutyric acid, *rac*-1.** Mp 172–173 °C. Lit.[13]: mp 176–177 °C. NMR spectra were identical with those cited above for (*R*)-**1**.

Solubility investigations. Filters Millipore 0.45 μm PTFE hydrophilic were used for the samples filtering. Micro syringes Hamilton (precision within ±1%) were used for analytical sampling and for adding fixed volumes of solvent. The mass of the samples was controlled with Sartorius CPA2P balance (accuracy ±1 μg).

The solubility of racemic and enantiopure samples was determined by chromatographic control of the concentration of saturated solution, equilibrious with the corresponding crystalline phase. For this purpose to pure acetonitrile (1mL) the corresponding solid phase was sequentially added by weighted portions with stirring until a stable turbidity of the liquid and the sediment at the bottom were observed. The total amount of the added substance was not less than 2 mg for racemate and 38 mg for enantiopure **1**. The vial was hermetically sealed by stopper and the slurry was stirred at a constant temperature (20 °C) during the day; the continual presence of the large excess of solid phase was monitored visually. After stopping the stirring and sedimentation, the liquid phase was sampled by syringe and filtered. An aliquot of the filtered solution (0.5 mL) was transferred to a test tube, and was diluted with methanol (0.5 mL). A solution of diazomethane in ether was added to the

aliquot until a stable light yellow coloration of the mixture. This is done to convert the free acid to the methyl ester, which is more convenient for subsequent chromatographic analysis. After 10 minutes the sample was evaporated to dryness *in vacuo*, the residue was dissolved in a fixed volume (1 mL) of isopropanol followed by a chromatographic determination of the substance concentration in the thus obtained sample. For the pre-calibration a series of accurately weighted samples of acid **1** (0.5-5 mg) was used, each of which, after dissolution in methanol, was subjected to a similar treatment (i.e. reaction with diazomethane, drying, dissolution in the precise volume of isopropanol).

Experiments were repeated twice; 2-3 chromatographic measurements were performed for each system. The absolute values of the solubility totaled 1.00(0.03) $g \cdot L^{-1}$ (or 4.49(0.15) $\cdot 10^{-3}$ $mole \cdot L^{-1}$) for *rac*-**1** and 25.4(1.1) $g \cdot L^{-1}$ (or 0.114(0.005) $mole \cdot L^{-1}$) for (*R*)-**1**.

To study the equilibrium solubility of the points of intermediate enantiomeric composition ($0 < ee < 1$) the series of (*R*)-**1** solutions in acetonitrile was prepared in first. The concentrations of enantiopure component within the series were *a fortiori* lower than its maximum solubility in acetonitrile, and ranged from 0.13 to 4 $mg \cdot mL^{-1}$. The solutions were prepared by serial dilution in half of aliquots of peak solution. In what follows, a fixed volume (1.5 mL) of one of thus prepared (*R*)-**1** solution was added to the weighed portion of *rac*-**1** (2 mg), the vials were sealed, and the mixture was stirred overnight at 20 °C until equilibrium was reached. Visual observation indicated the constant presence of a large excess of the solid phase in all samples. Selected values of the racemate mass, as well as the concentration and solution volume of the enantiopure substance, makes it possible to crystallize the solid phase in a wide range of enantiomeric compositions, including a hypothetical "anomalous conglomerate" 2:1.

After reaching equilibrium a liquid phase aliquot of each sample was filtered, treated with diazomethane and subjected to chromatographic analysis as described above. In addition to the total concentration of acid **1**, the equilibrium concentrations of individual stereoisomers in the liquid phase were determined in each of the experiments. To control the accuracy of the dilution

procedure, the preselected aliquots of stock solutions of all concentrations of enantiopure **1** were similarly analyzed.

The amount and composition of the equilibrium solid phase for each sample was calculated by difference in mass of the individual enantiomers in the racemate weighed portion and in the source and equilibrium solutions. It should be noted that for the determination of the composition of the solid phase, this technique proved to be more reproducible and accurate than the direct analysis of solids, as the latter inevitably entrains with itself a noticeable amount of solution, which significantly differs from solid by composition.

X-ray analysis. Both enantiopure and racemic samples of 4-benzoylamino-3-hydroxybutyric acid **1** were studied by single crystal X-ray analysis. The crystals of (*R*)-**1** for this purpose were grown by slow evaporation of the corresponding saturated solution in ethyl acetate; *rac*-**1** crystals were grown by two ways. Crystals having the form of flat prisms (see Figure 1a), were prepared by slow crystallization from concentrated water-free methanol solution on the interphase boundary with diethyl ether, taken in 5-fold excess. In the sequel, such crystals will be denoted as *rac*-**1.1**.

The second type of crystals, long needles (Figure 1b), were prepared by slow evaporation of concentrated solutions of the racemate in water. These crystals are referred to as *rac*-**1.2**.

The X-ray diffraction data of the investigated crystals were collected on a Bruker AXS Smart Apex II CCD ((*R*)-**1**, *rac*-**1.1**) and Bruker AXS Kappa Apex II CCD (*rac*-**1.2**) diffractometers in the ω- and θ-scan modes using graphite monochromated MoK_α (λ 0.71073 Å) radiation. The crystal data, data collection, and the refinement parameters are given in Table 1. Data were corrected for the absorption effect using SADABS program.[14] The structures were solved by direct method and refined by the full matrix least-squares using SHELXTL[15] and WinGX[16] programs. All non-hydrogen atoms were refined anisotropically. All hydrogen atoms were inserted at calculated positions and refined as riding atoms except the hydrogen atoms of NH and OH groups which were located from difference maps and refined isotropically.

All three crystals (*rac*-**1.1**. and *rac*-**1.2** samples were investigated at different temperatures) have very similar unit cell parameters, do not contain solvent molecules, and were solved in related spatial groups. Both racemic samples were refined in the centrosymmetric group *C*2/c. The structure of the enantiopure sample was solved and refined in Sohncke space groups *C*2. For reasons which we'll discuss later (see Results and Discussion) the attempts were made to solve the structures in the primitive triclinic cells *P*1 and *P*-1, which, however, did not lead to an improvement in the convergence parameters. Conversely, the model leads to disorder fragments in which the carboxyl groups are deployed at 180 degrees. In this regard, we believe that the option of solving and refinement the structures in base-centered monoclinic cells is more correct, as evidenced by the very good convergence parameters (see Table 1).

Data collections: images were indexed, integrated, and scaled using the APEX2[17] data reduction package. All Figures were made using Mercury program.[18] Molecular structures and conformations were analyzed by PLATON.[19] Crystallographic data (excluding structure factors) for the structures of (*R*)-**1,** *rac*-**1.1** and *rac*-**1.2** reported in this paper has been deposited with the Cambridge Crystallographic Data Centre as supplementary publication numbers CCDC 1036966-1036968 respectively. Copies of the data can be obtained, free of charge, on application to CCDC, 12 Union Road, Cambridge CB2 1EZ, UK, (fax: +44-(0)1223-336033 or e-mail: deposit@ccdc.cam.ac.uk).

The X-ray phase studies for the compound **1** polycrystalline samples were performed on a Bruker D8 Advance diffractometer equipped with Vario attachment and Vantec linear PSD, using Cu radiation (40 kV, 40 mA) monochromated by the curved Johansson monochromator (λ Cu $K_{\alpha 1}$ 1.5406 Å). Room-temperature data were collected in the reflection mode with a flat-plate sample. The samples were loaded on a silicon plate reducing background scattering. Patterns were recorded in the 2Θ range between 3^{o} and 60^{o}, in 0.008^{o} steps, with a step time of 0.1 - 0.5 s.

Table 1. Crystallographic Data for Crystalline Compounds *rac*-1 and (*R*)-1

Compound, sample	*rac*-**1.1**	*rac*-**1.2**	(*R*)-**1**
Formula	$C_{11}H_{13}NO_4$	$C_{11}H_{13}NO_4$	$C_{11}H_{13}NO_4$
M (g/mol)	223.22	223.22	223.22
Temperature, K	151(2)	296(2)	150(2)
Crystal class	Monoclinic	Monoclinic	Monoclinic
Space group	*C*2/c	*C*2/c	*C*2
Crystal size	0.22×0.20×0.10 mm^3	0.38×0.18×0.14 mm^3	0.58×0.53×0.04 mm^3
Z, Z′	8, 1	8, 1	8, 2
Cell parameters	*a* = 24.794(5) Å, *b* = 11.355(2) Å, *c* = 7.7615(14) Å β = 97.727(2)°	*a* = 24.64(1) *b* = 11.524(5) *c* = 7.871(4) β = 98.24(1)	*a* = 24.355(6) Å, *b* = 11.626(3) Å, *c* = 7.783(2) Å β = 98.371(3)°
V, $Å^3$	2165.4(7)	2212(2)	2180(1)
F(000)	944	944	944
ρ_{calc}, g/cm^3	1.369	1.340	1.360
μ, cm^{-1}	1.05	1.03	1.04
θ, deg	3.07≤ θ ≤ 30.42	4.26≤ θ ≤ 27.93	1.94≤ θ ≤ 29.38
Reflections measured	10479	9457	10932
Independent reflections	2752 [*R*(int) = 0.0226]	2583 [*R*(int) = 0.0725]	5006 [*R*(int) = 0.0199]
Number of parameters / restraints	156/1	151/0	314 / 1
Reflections [$I > 2\sigma(I)$]	2335	1405	4688
R_1 / wR_2 [$I > 2\sigma(I)$]	0.0517/ 0.1305	0.0626/ 0.1506	0.0332/ 0.0778
R_1 / wR_2 (all reflections)	0.0604 / 0.1374	0.1225/ 0.1830	0.0367 / 0.0802
Goodness-of-fit on F^2	1.029	0.979	1.032
ρ_{max}/ρ_{min} ($eÅ^{-3}$)	0.542 / -0.432	0.309 / -0.277	0.352 / -0.276

RESULTS AND DISCUSSION

Synthesis. Preparation of the necessary for our research enantiopure and racemic samples of 4-benzylamino-3-hydroxybutyric acid **1** is shown in Scheme 3.

Scheme 3. Preparation of racemic and enantiopure samples **1**

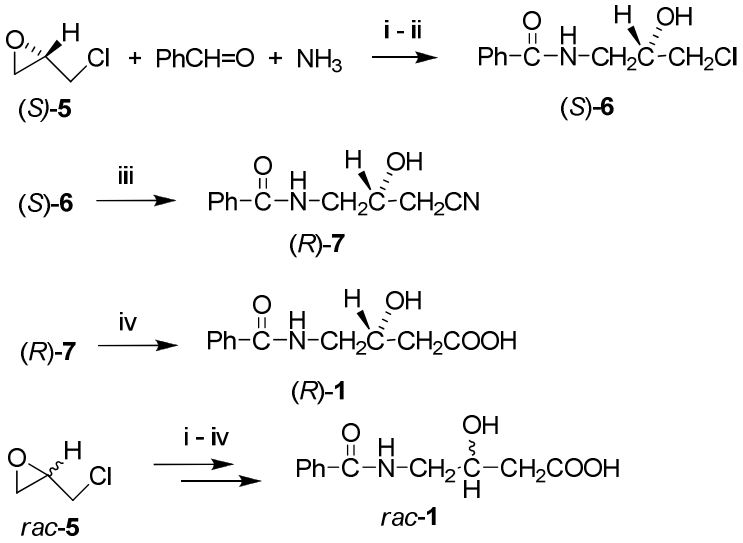

Reagents and conditions: (*i*) (*S*)-epichlorohydrin (1 eq, 96 % ee), benzaldehyde (1 eq), aqueous NH_3 (26 wt%, 1.7 eq), ethanol; (*ii*) PhC(O)Cl (1 eq), Py (1 eq), $CHCl_3$, -40 ^oC; (*iii*) NaCN (1.6 eq), KI (0.019 eq), aqueous ethanol (67%), >99% ee; (*iv*) 3N NaOH, H_2O_2, 63-65 ^oC, 98% ee.

As a source of chirality for (*R*)-**1** an enantiopure epichlorohydrin (*S*)-**5** was used. Condensation of the latter with benzaldehyde and ammonia and subsequent treatment of the condensation products with benzoyl chloride in dry pyridine yielded the chloromethyl derivative (*S*)-**6**, which in turn was converted to enantiopure nitrile (*R*)-**7**. This synthetic route is based on the modified literature procedures for the synthesis of the racemic products reported by Mazetti and Lemmon.[20] However, we found that the original literature procedure utilizing hydrolysis of boiling nitrile **7** with aqueous HBr leads to a complete hydrolysis of the product to 3-amino-2-hydroxybutyric acid. Therefore, we developed here the optimized procedure using a soft alkaline hydrolysis in the presence of hydrogen peroxide, as proposed in reference[21] for labile nitriles. The same sequence of synthetic transformations of racemic epichlorohydrin *rac*-**5** was used in this work to obtain a sample of *rac*-**1**.

Crystal habit and IR spectra comparison for (*R*)-1 and *rac*-1 crystals. Amino acid **1** is composed of hydrophobic (phenyl ring) and hydrophilic (carboxy, hydroxy and amino) fragments. Therefore, it is soluble in organic solvents and in water. Figure 1 shows micrographs of crystals of racemic and enantiopure amino acids **1** grown by us from an organic solvent (see Experimental Section) and water.

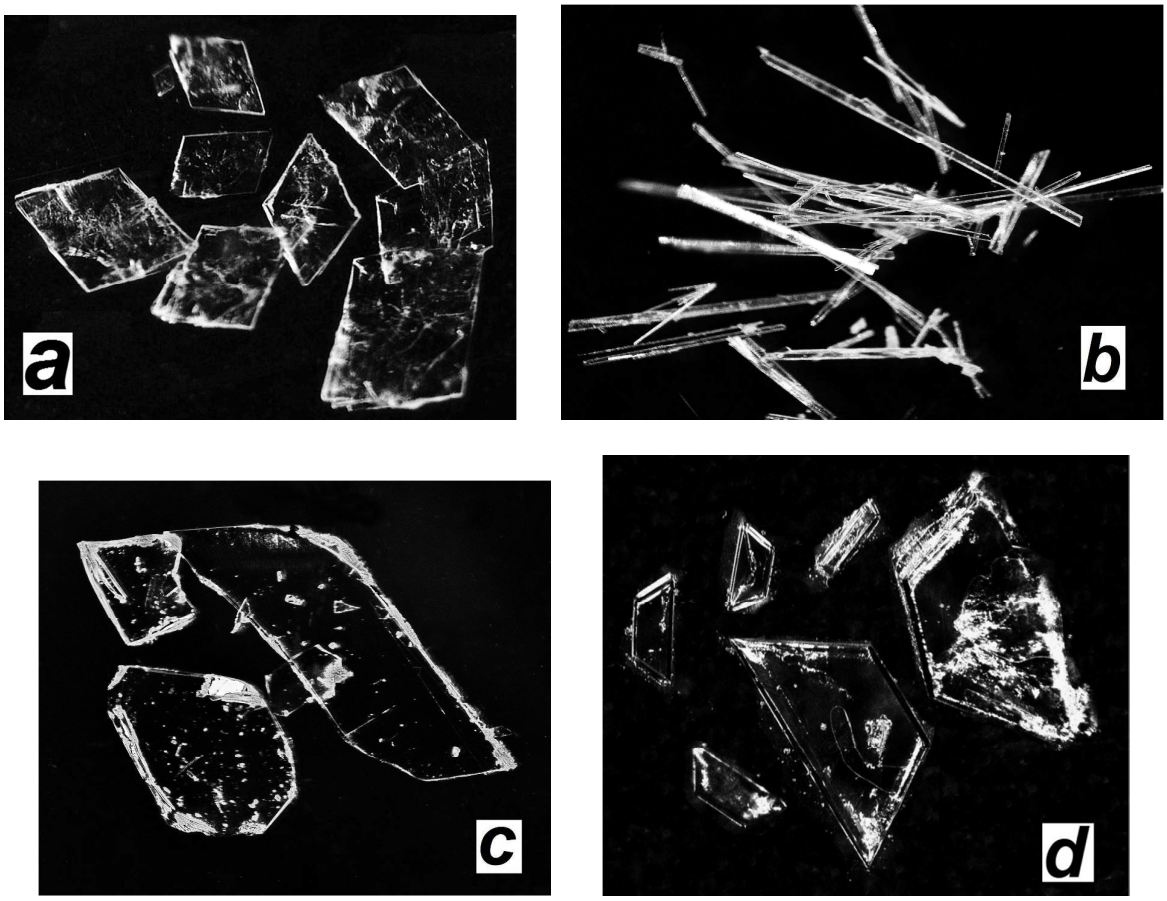

Figure 1. Microscopic pictures of the racemic and homochiral samples of compound **1**. (**a**) Thin prisms of *rac*-**1.1** from organic solvent; (**b**) needle-like crystals of *rac*-**1.2** from water; plates of (*R*)-**1** both from organic medium (**c**) and water (**d**).

The paper[1] states that the homochiral sample is crystallized from water as a solvate with one molecule of water. According to the authors, this crystal modification has mp = 78–81 °C. At the same time the racemate crystals do not form hydrates. Figure 1 show that the essential difference between the appearance of the crystals, prepared from organic and aqueous medium, is

characteristic only for the racemate. The crystals grown at the interface of methanol and ether (see Experimental Section) comprise flat transparent good faceted prisms (Figure 1a), whereas the ones, precipitated from water, have elongated needle-like form (Figure 1b). Crystals of the acid (*R*)-**1** grown from ethyl acetate constitute poorly faceted plates (Figure 1c). The enantiopure sample crystallizes from water as thin trapezoids (Figure 1d). We note here that the crystals obtained from different medium have (in pairs) similar melting points, namely 114–116 °C for (*R*)-**1** and 172–173 °C for *rac*-**1**.

When the crystal forming molecules are identical (up to mirroring), the simplest procedure to detect similarities and differences of the crystal structure is a comparison of their vibrational spectra. For the purpose of establishing of the reliable criteria of the similarities and differences of complex spectral curves, we have previously proposed to use the standard Pearson correlation coefficient **r** between two digital arrays (A_i,v_i), where ν_i stands for the vibration frequency (usually expressed in wave numbers in increments of 1 cm^{-1}), and A_i corresponds to the extinction at this wave number.[22] To allow for a more detailed visual comparison of the vibration spectra, we proposed to use a graphical representation of the correlation between the two spectra, that is, visually display them in the coordinates A_i^1 versus A_i^2. In the case of perfect coincidence (identity) of the spectra, the correlation trajectory degenerates into the first diagonal. Partial mismatch between the spectra in frequencies, intensity, baseline drift, the presence of impurities in the sample and/or matrix, or the like, results in a deviation from the diagonal trajectory, and is described in a very characteristic way for each type of distinctions. The details of this approach have been described in our recent paper.[23]

Comparison of the IR spectra for compound **1** crystalline samples is shown in Figure 2. As can be seen from Figures 2a and 2b, the spectra of different (*R*)-**1** crystalline samples perfectly correlated (**r** = 0.998), correlation trajectory is compact and practically coincides with the main diagonal. To grow the crystals depicted in Figure 1c, the anhydrous solvent was used, and the melting point of both types of (*R*)-**1** crystals coincides with the literature data for the anhydrous

samples. This means that the Bergman's and Lissitzin's information that the enantiopure acid precipitates from water in the form of the monohydrate (*R*)-**1**·H_2O, [1] is most likely erroneous, and enantiopure samples of 1 grown from the organic and aqueous medium are identical. For this reason, only one crystal grown from the organic solvent was examined by a single crystal X-ray analysis (see below).

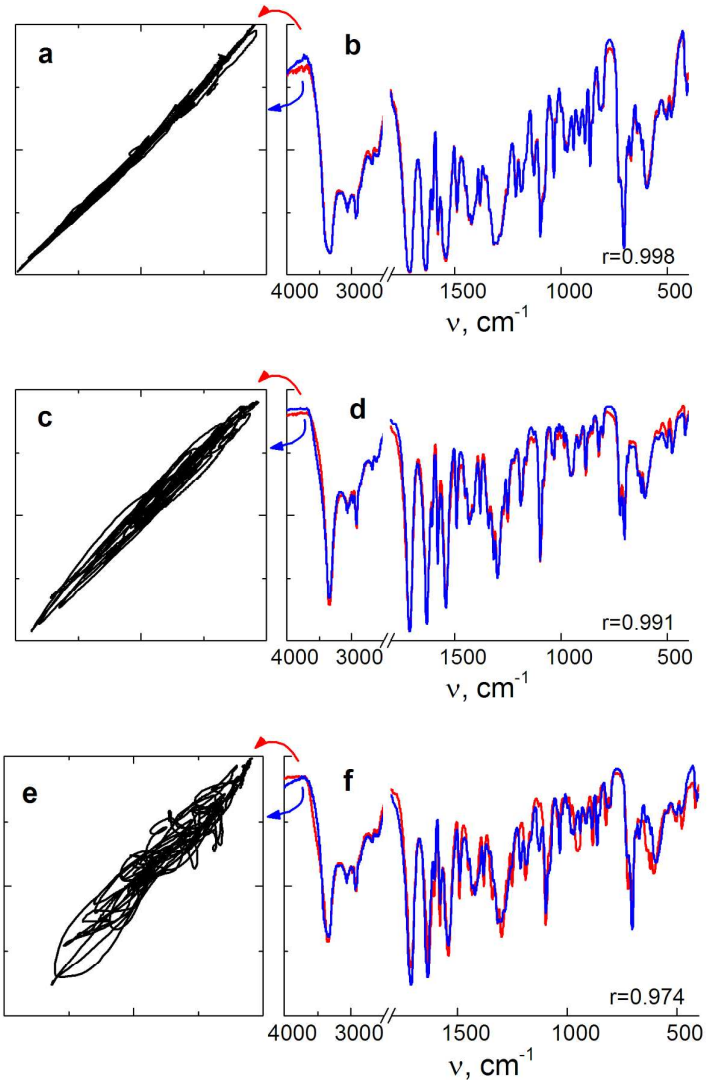

Figure 2. Correlation trajectories (**a,c,e**) for IR spectra in KBr pellets (**b,d,f**) of the pair of crystals: (*R*)-**1** from water (red curve) against (*R*)-**1** from ethyl acetate (blue curve) (**a**,**b**); *rac*-**1** from water (red curve) against *rac*-**1** from methanol/ether (blue curve) (**c,d**); *rac*-**1** from methanol/ether (red curve) against (*R*)-**1** from ethyl acetate (blue curve) (**e,f**).

The vibrational spectra of the racemic crystals also correlate quite well with each other (Figure 2c,d), however the correlation coefficient, **r** = 0.991, decreases somewhat. Nevertheless, the

correlation trajectory is not as compact as for a pair of (*R*)-**1** crystals. The most distinct differences are manifested in the region of $\nu_{OH} \sim 3450$ cm^{-1}. It can be assumed that these differences are not associated with the internal crystal structure, but with the crystal habit. However, to avoid ambiguity, both types of crystals have been studied by X-ray diffraction; the samples were tested at various temperatures during the analysis (Table. 1).

As seen from Figure 2f, there are significant differences between the spectra of racemic (red curve) and enantiopure (blue curve) samples of **1** (for comparison were used samples grown from the organic medium); and the correlation coefficient **r** = 0.984 between the arrays A_i^R and A_i^A (here and hereinafter *R* and *A* upper indices stand for the racemic and enantiopure samples) is relatively poor. The corresponding correlation trajectory for the two spectra is shown in Figure 2e. In general, the "fuzzy" image presented in Figure 2e is typical for poor-correlated spectra.

The discrepancy between the IR spectra of crystals of racemic and homochiral samples allows to reject the possibility of **1** to crystallize in the form of normal conglomerate. But the rest of the crystallographic possibilities at this stage remain open. Further investigation of the phase behavior of amino acid **1** was performed by means of single crystal X-ray investigations.

Single crystal X-ray investigations. Before proceeding to describe the crystal structure of the investigated samples, we note one important fact. As mentioned in the experimental part, the hydrogen atoms of NH and OH groups were located from difference maps and refined isotropically with sufficiently good convergence parameters (Table 1). Within the all structures the carboxyl moieties of adjacent molecules form intermolecular hydrogen bonds, leading to dimeric structures, which are typical of carboxylic acids in crystals. In principle, such a H-dimer may be (a) located in the general position; (b) formed around the twofold rotation axis, orthogonal to the H-bonds plane; (c) formed around a center of symmetry lying in the hydrogen bonds plane; (d) located on the twofold rotation axis, lying in-plane of H-bonds. Typically, variants (b) and/or (c) are realized in the crystals of carboxylic acids, which results in the well-known cyclic supramolecular synthon denoted as a "fork" H-dimer (or "anti-dimer" on the Scheme 4). In our case only the option (d) does not lead

to conflicts with the existing *C*2 or *C*2/c lattice symmetry elements. For this reason, for all the studied samples the primary structure solution (in which all atoms are in general position) led to the dimers, indicated as "syn-dimers" in Scheme 4.

Scheme 4. "Anti-" and "syn-dimers" of carbonic acids

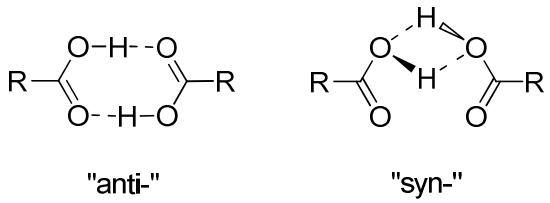

Our turning to Cambridge Crystallographic Database showed that "syn-dimers" of carboxylic acids with noncentro-symmetrical arrangement of the hydroxyl groups are fairly common, though, of course, do not dominate. Our selective analysis of both "right" and "wrong" structures showed that the problem of the correct determination of the position of the hydrogen atoms of the hydroxyl group in the carboxyl moiety of carboxylic acid dimers is a serious problem, which requires a special consideration. However, it is beyond the scope of the problems addressed in this paper. We hope that soon we will present the results of our analysis of this phenomenon in a separate publication.

In this work, we prefer to deal with a more conventional "anti-dimer" ("fork" H-dimer). For this purpose, the hydrogen atoms of hydroxyl groups in the carboxyl fragments during the refinement were fixed in special position on the twofold axis, and the distances O-H and O···H in "anti-dimers" are aligned in pairs, i.e. receive the same value in each triad O···H···O but different for those fragments which are not connected by symmetry. The characteristics obtained for this model of refinement are discussed below. Note that, except for the carboxyl moieties themselves, they remain substantially constant for the other mentioned refinement modes.

Racemic sample *rac*-**1.1**, grown in an organic medium (Figure 1a) crystallizes with one molecule in the asymmetric unit of a base-centered monoclinic cell. The geometry of the molecule and partial numbering scheme (common to all subsequent molecules studied in this work) are shown in Figure

3. The bond lengths and angles are within the range of expected average values for organic compounds. The most important result in the context of our study is that the sample crystallizes in the "non-Sohncke" space group C2/c. Consequently, *rac*-**1.1** crystals present a normal racemic compound which contains an equal amount of both enantiomers in the unit cell.

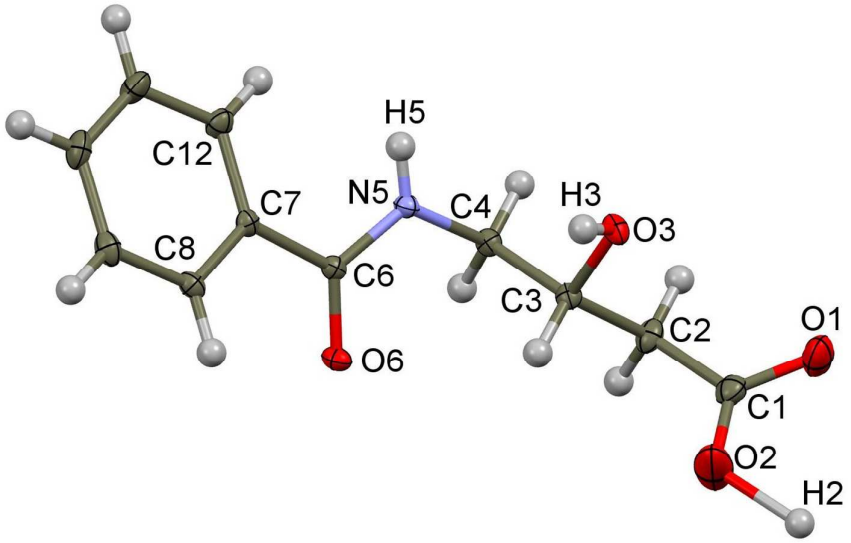

Figure 3. ORTEP plot of the molecule in the crystals of *rac*-**1.1** and the partial numbering scheme adopted for the molecules **1** in the present work. Displacement ellipsoids are drawn at the 50% probability level, hydrogen atoms are represented as fixed-size spheres.

The crystal structure of the sample *rac*-**1.2** (Figure 1b) is very close to those for the sample *rac*-**1.1** (Table 1), although they were obtained at significantly different temperatures. This confirms the above conclusion about the similarity of the crystal structure of *rac*-**1** samples grown in aqueous and organic medium. Simultaneously, the data obtained allow making some assumptions about such a pronounced environment effect on the habit of racemic crystals.

Figure 4 shows the Miller indices for some crystal faces. As follows from the figure, for all the studied crystals the faces of the smallest growth are the base planes [100] and [-100], thus a crystal growth is carried out mainly in the tangential directions. Although the quality of the faceting does not always allow to accurately determine the preferential direction among them. The significant difference of crystals of the racemic sample, prepared from an aqueous solution, is to block the

growth of faces belonging to the second basic direction 010, so that the main growth occurs along the directions close to the third base vector 001. It is of interest to note, that in *rac*-**1** crystals the centrosymmetric intermolecular hydrogen bonds N–H···OH, through which one-dimensional supramolecular associates (columns) are linked into 3D supramolecular packing (see below), are oriented approximately in the same 010 direction. Based on these considerations, the competitive participation of water molecules in the formation of hydrogen bonds with the amino groups likely disables the growth of one of the faces of the crystals. Of course, due to recombination processes, the growth of the corresponding faces does not stop completely, but noticeably slows down, which in the long run may cause the formation of needle-shaped crystals.

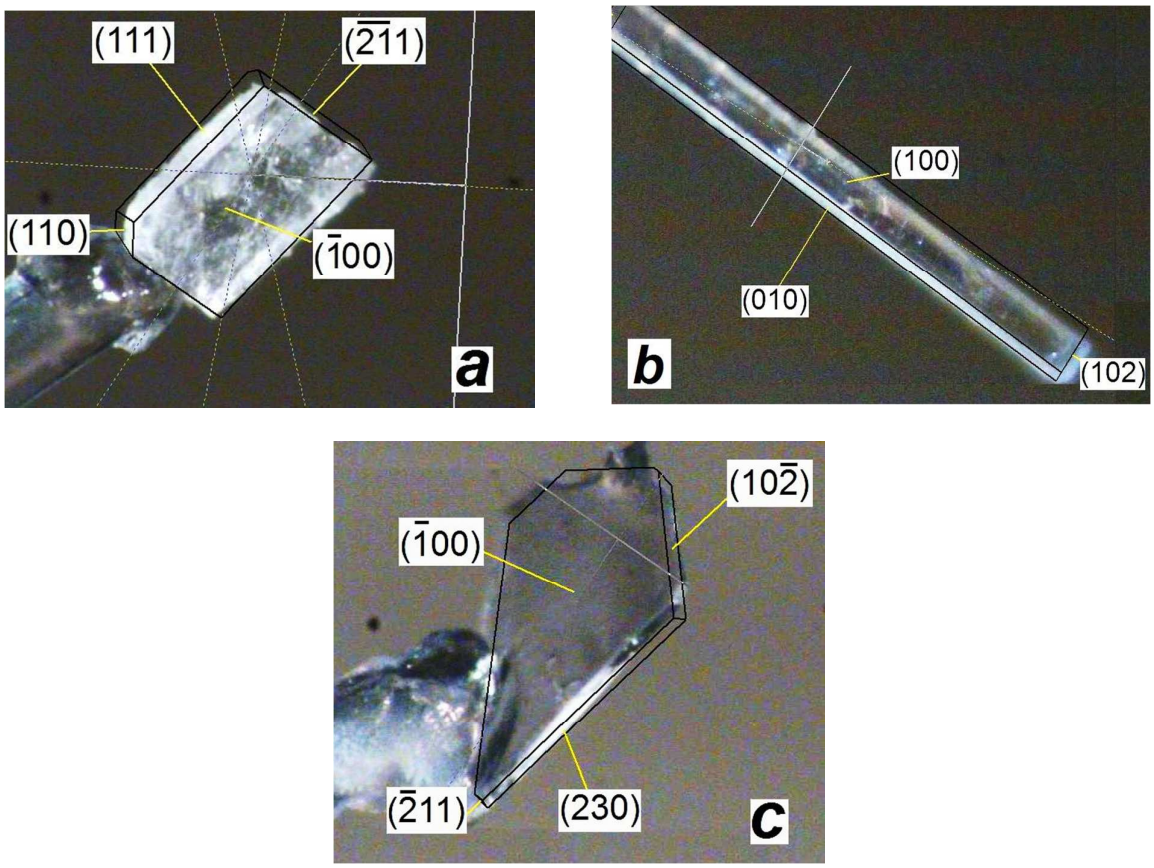

Figure 4. Miller indices of crystal faces of the *rac*-**1.1** (a), *rac*-**1.2** (b), and (*R*)-**1** (c) crystals.

Supramolecular structure in the *rac*-**1.1** crystal (the same as for crystals of *rac*-**1.2**) is determined by the combined action of the classical intermolecular hydrogen bonds O–H···O and N–H···O (Table 2). Crystals also include weaker C–H ···O interaction acting primarily in the same directions.

Table 2. Parameters of the classical intermolecular H-bonds for *rac*-1.1 crystals

D–H···A	D–H, Å	H···A, Å	D···A, Å	∠ DHA, °	Symmetry operation
O2-H2···O2”	1.421(2)	1.421(2)	2.841(4)	179(2)	2-x,y,1/2-z (2-fold axis)
O1-H2’···O1”	1.42(2)	1.42(2)	2.597(2)	132 (2)	2-x,y,1/2-z (2-fold axis)
O3-H3···O6”’	0.86(2)	1.90(2)	2.736(1)	165(2)	x,-y,1/2+z
N5-H5···O3””	0.82(2)	2.21(2)	2.969(1)	154(2)	3/2-x,1/2-y,-z

In the analysis of the crystal structure of *rac*-**1** as the initial zero-dimensional supramolecular unit one can take the localized "fork" dimer, the molecules of which are physically linked through intermolecular H-bonds between the carboxyl groups and are symmetrically related by simple rotary axes (Figure 5a). These dimers can be formed only by molecules with the same configuration of the chiral centers (Figure 5a).

The molecules, constituent of the nearby enantiomeric "fork" dimers, are linked through the pairs of classical hydrogen bonds O3–H3···O6=C6 obeying the central symmetry. The arising supramolecular structure presents a one-dimensional column oriented along *0c* axis (Figure 5b,c). In the crystal, each such column (e.g., column, indicated in gray in Figure 5d) is surrounded by six the same ones (these columns are color-coded in the figure). In addition, each 1D column is linked to four adjacent columns through the system of the spreading along *0c* direction centrosymmetric intermolecular bonds N–H···OH (in Figure 5d they are marked with red dashed lines). Thus constructed packing of the racemic compound is sufficiently dense (PI = 70.4%) and contains no voids, potentially available for the molecules of a solvent.

Enantiopure (*R*)-**1** sample crystallizes with two molecules per asymmetric unit of base-centered monoclinic cell (space group *C*2). Increasing the number of symmetrically independent molecules (parameter Z') when moving from a racemic to the enantiomeric sample is common for carboxylic

acids. As shown by Steed et al., this fact is related to the dimeric nature of their supramolecular synthon.[24] Comparative analysis reveals a striking similarity between the unit cell parameters for (*R*)-**1** and *rac*-**1** (Table 1). Taking into account that the group *C*2 is a subgroup of *C*2/c, we can expect that the packing nature of homo- and heterochiral crystals would be close to one another.

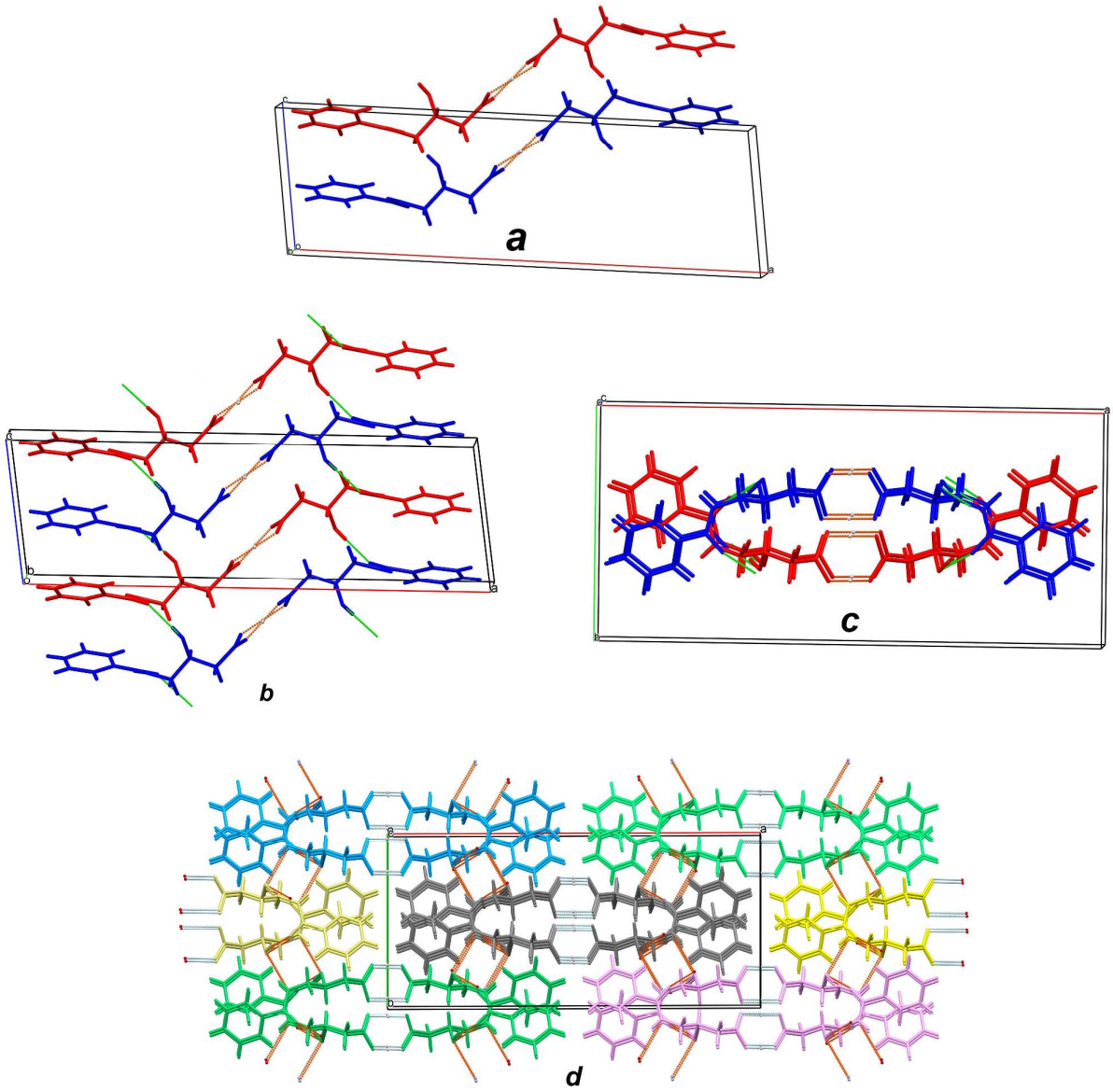

Figure 5. Supramolecular crystal structure of *rac*-**1**. (**a**) Zero-dimensional enantiomeric "fork" dimers; view along the *0b* axis. Hereinafter dotted lines denote the intermolecular hydrogen bonds (IMHB); (*R*)-enantiomers colored in red, (*S*)-enantiomers – in blue. (**b**) The 1D column of "fork" dimers joined by IMHB O–H···O=C (labeled green); view along the *0b* axis. (**c**) The same column;

view along the *0c* axis. (**d**) Merging of the one-dimensional columns into a three-dimensional supramolecular structure through IMHB NH···OH (marked in red); view along the *0c* axis.

Symmetrically independent molecules A and B have an identical configuration and close values of bond lengths and bond angles. Visually, the structures of these molecules are compared in Figure 6a.

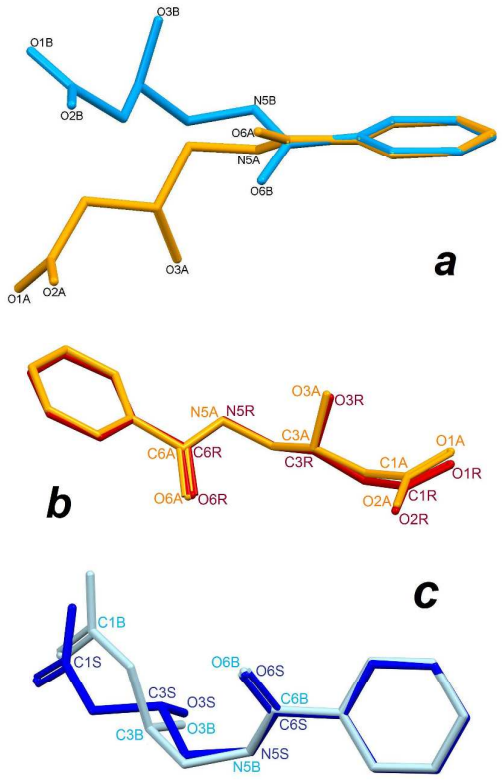

Figure 6. Conditional superposition of the molecules existing in the amino acid **1** crystals. (**a**) Two independent molecules, A (orange) and B (light blue), in the crystal of (*R*)-**1**. (**b**) Molecule A (orange) in (*R*)-**1** crystal and molecule of *R*-enantiomer (red) in the crystals of *rac*-**1**. (**c**) Molecule B (light blue) in (*R*)-**1** crystal and molecule of (*S*)-enantiomer (blue) in the crystals of *rac*-**1**.

More specifically, the conformations of the molecules **1** in crystals are characterized by torsion angles listed in Table 3. For ease of comparison, this table also shows torsion angles for the two enantiomers in the *rac*-**1.1** crystals. The table shows that the torsion angles of molecule A in the (*R*)-**1** crystals, by the absolute values and by the signs, are practically identical with those of the independent molecules having *R*-configuration in *rac*-**1.1** crystal. (The virtual distinction for torsion angles N5C4C3C2 must not be misleading: in both cases we are dealing with antiperiplanar

orientation of N5-C4 and C3-C2 bonds, and the actual difference in the dihedral angles of only about 5 °.) Visually, this similarity can be clearly seen in Figure 6b.

Table 3. **Main torsion angles for the molecules 1 in (*R*)-1 and *rac*-1.1 crystals**

Torsion angle (°)	(*R*)-**1** sample		*rac*-**1.1** sample	
	A molecule	**B** molecule	*R*-enantiomer	*S*-enantiomer
C8C7C6N5	-155.22	156.02	-157.05	157.05
C8C7C6O6	24.88	-24.59	22.97	-22.97
C7C6N5C4	-175.00	164.90	-174.93	174.93
C6N5C4C3	-84.14	91.42	-79.25	79.25
N5C4C3C2	-177.81	-84.40	177.35	-177.35
N5C4C3O3	-60.75	42.00	-64.33	64.33
C4C3C2C1	-179.30	-176.24	-179.89	179.89
C3C2C1O1	-119.95	-162.06	-118.00	118.00
C3C2C1O2	60.69	23.14	59.70	-59.70

At the same time, the torsion angles for independent B molecule, which naturally has the *R*-configuration in the crystal of (*R*)-**1**, are more similar to the torsion angles of *S*-enantiomer in the *rac*-**1.1** crystal. The impression arises (see Figure 6c) that the independent molecule B mimics the molecule of (*S*)-enantiomer, which is absent in the real homochiral crystal. This impression is enhanced in the analysis of the intermolecular hydrogen bonds (Table 4) and supramolecular packing details in the crystals of (*R*)-**1**.

Table 4. Parameters of the intermolecular H-bonds for (*R*)-1 crystals

D–H···A	D–H, Å	H···A, Å	D···A, Å	∠ DHA, °	Symmetry operation
O2A-H2A···O2A”	1.341(5)	1.341(5)	2.674(2)	170(2)	-x,y,-z (2-fold axis)
O1A-H2A’···O1A”	1.289(7)	1.289(7)	2.567(2)	169(2)	-x,y,-z (2-fold axis)
O2B-H2B···O2B”’	1.308(6)	1.308(6)	2.609(3)	172(2)	1-x,y,1-z (2-fold axis)
O1B-H2B’···O1B”’	1.390(6)	1.390(6)	2.778(2)	175(2)	1-x,y,1-z (2-fold axis)
O3A-H3A···O6B*	0.83(2)	1.91(2)	2.719(1)	167(2)	1/2-x,-1/2+y,-z
O3B-H3B···O6A**	0.82(2)	2.06(2)	2.811(2)	153(2)	1/2-x,1/2+y,1-z
N5A-H5A···O3B	0.85(2)	2.09(1)	2.903(2)	159(2)	-
N5B-H5B···O3A	0.86(2)	2.21(2)	2.947(2)	144(1)	-

Thus, independent molecules A and B in the (*R*)-**1** crystals are merged in "fork" H-dimers around simple rotary axes of order 2. These H-dimers, A···A and B···B, are analogues of homochiral dimers R···R and S···S in the *rac*-**1** crystals. Next, the dimers A···A and B···B in the (*R*)-**1** crystals are bound through the system of IMHB O3–H3···O6=C6 in one-dimensional columns (Figure 7) which are very similar with the one-dimensional columns in the *rac*-**1** crystals (Figure 5c). Here the role of *R*-enantiomer is played by the molecule A, and the molecule B plays the role of *S*-enantiomer. Finally, four of the six contiguous columns are merged in 3D crystal structure with the particular 1D column through the channel system of IMHB N–H···OH (indicated by red dashed rays in Figure 7).

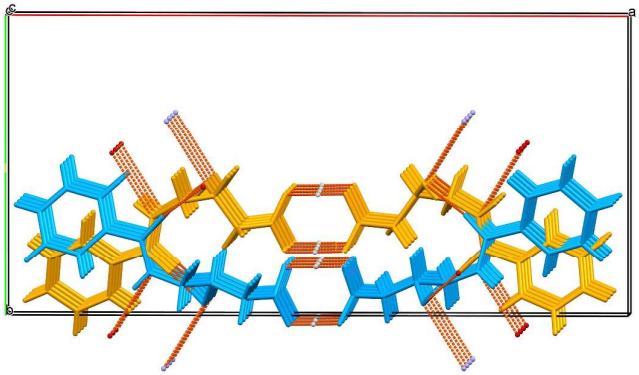

Figure 7. 1D column formed by independent molecules A and B in the crystals of (*R*)-**1**. View along *0c* axis.

On the whole, judging from the calculated value of the packing index equal 69.3%, so constructed crystal packing is sufficiently dense. Nevertheless, it is possible to name at least three reasons, according to which the homochiral crystal packing should be less advantageous than heterochiral one. Firstly, *two* symmetry independent molecules participate in the formation of homochiral crystal instead of *one* in the case of racemic crystal. Secondly, the conformation sequence for the main chain of nonhydrogen atoms C8C7C6N5C4C3C2C1 in *S*-enantiomer in a racemic crystal is described by the formula *ap,ap,sc,ap,ap*, while the conformation of independent B molecule, which simulates the *S*-enantiomer in homochiral crystal, is described by formula *ap,ac,ort,-ort,ap*, where at least two sterically optimal antiperiplanar moieties are replaced by two less favorable anticlinal and orthogonal fragments. Third, for some crystal forming intermolecular classical hydrogen bonds

in the (*R*)-**1** crystal (Table 4), the angular characteristics (∠DHA) are changed for the worse in comparison with the same in the *rac*-**1.1** crystal (Table 2).

Before leaving the section associated with the X-ray analysis of amino acid **1** crystals, we would like to make one more remark. Based on our previous studies of a series of glycerol ethers, we established the relationship between the orientation of supramolecular structures and unit cell parameters and found that the direction of the strongest crystal forming interaction corresponds to the smallest unit cell parameter.[9] In the case of compound **1**, the smallest parameter is the *c* axis, – followed by the *b* axis. Therefore, we can assume that the strongest interactions in our systems are formed by paired hydrogen bonds O–H···O=C propagating along the direction of *0c*. Next in force are hydrogen bonds N-H···OH oriented along *0b*. Finally, the localized IMHB are oriented along the longest *a* axis, forming "fork" dimers; these interactions have a minimal impact on the formation of a general supramolecular structure of the crystals.

Solubility and ternary phase diagram. Thus, X-ray analysis showed that, at least from a racemic solution, the amino acid **1** is crystallized in the form of a normal racemic compound. In addition, the crystals of the racemic compound (as well as homochiral crystals) do not contain voids in their structure available for solvent molecules. Finally, we examined a quantitative dependence of the solubility of compound **1** on the enantiomeric composition of the solid phase, which is present in equilibrium with the solution. This kind of study allowed us to construct the ternary phase diagram of the solubility of the system and thus to establish the number and nature of the phases formed by it and to identify the areas of their (phases) stability and some thermodynamic parameters of the interfacial equilibria.

We used an achiral acetonitrile as a solvent in our study, since it is chemically stable, does not form crystal solvates with the system components and provides acceptable solubility measurement intervals. In our work, we restricted ourselves to isothermal measurements at 20 ± 0°C.

The equilibrium solubility of racemic and enantiopure samples of **1**, i.e. saturated solution concentration in equilibrium with the corresponding crystalline phase, C_{sat}, was determined by

liquid chromatography as described in the Experimental section. The values obtained were equal C_{sat}^{R} = 4.49·10^{-3} mole·L^{-1} for *rac*-**1** and C_{sat}^{A} = 0.114 mole·L^{-1} for (*R*)-**1**. Generally speaking, the difference in solubility of the homochiral and racemic samples was observed by our predecessors.[1] Moreover, the solubility of an enantiopure substance typically exceeds the solubility of a racemate 2-10 times.[25,26] Here we emphasize that for the amino acids **1** these differences (about 25 times!) are abnormally large.

When studying the equilibrium solubility of solid samples of intermediate enantiomeric composition (0 < ee < 1), it is necessary to control not only the concentration and enantiomeric composition of the obtained solution, but also the resulting composition of the solid phase, which was retained after reaching equilibrium, because it may differ from the initial composition (before addition of solvent). The details of quantitative chromatographic measurements are given in the Experimental section. The measurement results are shown in Table 5 and Figure 8. In Figure 9 the data are represented as a fragment of the ternary phase diagram of the system.

Table 5. Equilibrium composition of the solid and liquid phases of saturated solutions of 4-benzoylamino-3-hydroxybutyric acid 1 in acetonitrile

sample index	[C_R] in liquid phase, mole·L^{-1}, ×10^3	[C_S] in liquid phase, mole·L^{-1}, ×10^3	mole fraction of (*R*)-**1** in liquid phase	mole fraction of (*R*)-**1** in solid phase
1	2.25	2.25	0.50	0.50
2	2.18	1.63	0.57	0.50
3	2.65	1.54	0.63	0.50
4	3.47	1.27	0.73	0.51
5	4.85	0.80	0.86	0.53
6	9.97	0.49	0.95	0.48
7	18.0	0.18	0.99	0.53
8	114	-	1.00	1.00

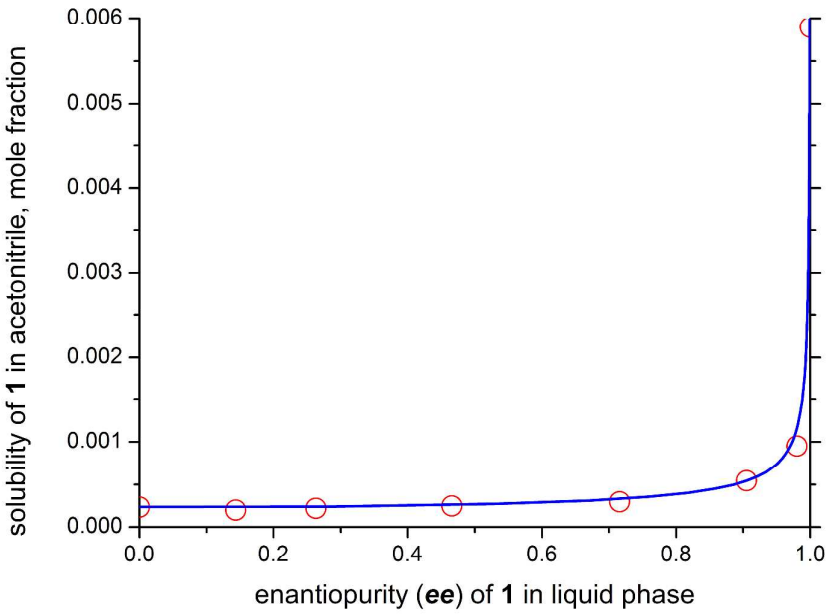

Figure 8. The dependence between the amino acid **1** solubility in acetonitrile and the enantiomeric excess of **1** in solution. Red circles - the experimental solubility values, blue curve - the values calculated under the assumption that the single racemic compound is formed in the system.

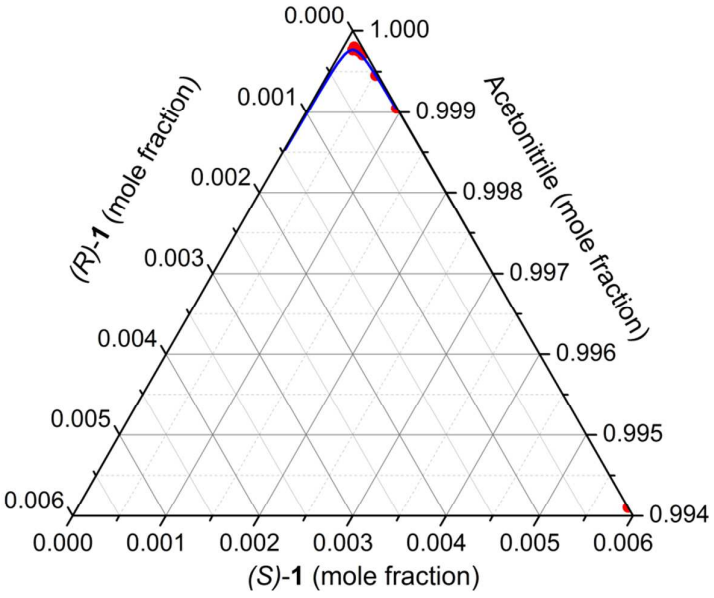

Figure 9. Ternary phase solubility diagram (fragment) in the system CH_3CN/(*R*)-**1**/(*S*)-**1**. Red circles - the experimental values of the equilibrium composition of the liquid phase.

As evidenced by Figure 8, the experimental points corresponding to the equilibrium composition of the liquid phase (red circles) are visually situated on a monotonic curve, which does not contain discontinuities or extrema, when the enantiomeric composition of the liquid phase lies within the range of ee = 0.5÷0.98. Therewith, in this range of the compositions of the liquid phase, which is in equilibrium with the solid phase, the enantiomeric composition of the solid remains almost unchanged and corresponds to racemate within an experimental error (see Table 5, 5th column). These features reliably indicate that in the investigated range of compositions the only equilibrium that exists in this system is between the solution and a crystalline 1:1 racemic compound. Thus the investigated interval belongs to the branch of the ternary phase diagram contained between pure racemic compound and its eutectic with enantiopure substance. If this is true, then the liquidus line in this range should be described by the solubility product (SP) for normal racemic compound

$$[R] \cdot [S] = SP = const \qquad (1).$$

Numerical *SP* value may be found on the basis of the solubility of pure racemic compound. Since for such a system

$$[R^R] = [S^R] = \frac{1}{2C_{sat}^R} \qquad (2),$$

then

$$SP = (1/2C_{sat}^R)^2 \qquad (3).$$

The blue curve in Figure 8 is the liquidus line, calculated on the basis of equation (1) after the substitution of the numerical value of $SP = 5.04 \cdot 10^{-6}$ mole$^2 \cdot$L^{-2}, found from equation 3, after the substitution of the experimental value of C_{sat}^R. Figure 8 shows that the points, corresponding to the experimentally observed values of the equilibrium composition of the liquid phase, fit well the theoretical curve. This suggests that the phase diagram of the system is exhaustively described by the equilibrium between a solution, a racemic 1:1 compound, and an enantiopure substance. The phase diagram has no zones of solid solutions, and no molecular addition compounds of intermediate composition are formed in the system. Consequently, in the equilibrium conditions the

existence of the crystalline molecular compound 2:1, postulated by Bergman and Lissitzin,[1] is impossible.

Normal racemic compounds refer to simple eutectic systems, in which the solid eutectic is formed by individual phases of the racemic compound and the predominant enantiomer (for clarity, arbitrarily denoted by symbol *R*). In the solid state, the activity of the pure substance forming the individual phase is unity. For the solution in equilibrium with the solid phase, the activities of both (liquid and solid) components are equal. Consequently, the activity of the dominant enantiomer in solution in equilibrium with the eutectic is also equal to one. For a dilute solution the activity can be replaced of the concentration, and then the enantiomeric composition of the eutectic could be easily found according to the following scheme:[27,28]

$$ee_{eu} = \frac{[R^{eu}] - [S^{eu}]}{[R^{eu}] + [S^{eu}]}$$

$$[R^{eu}][S^{eu}] = SP = (1/2C^{R}_{sat})^2$$

$$[R^{eu}] = C^{A}_{sat}$$

$$[S^{eu}] = \frac{(1/2C^{R}_{sat})^2}{C^{A}_{sat}}$$

$$ee_{eu} = \frac{1 - \left(\frac{C^{R}_{sat}}{2C^{A}_{sat}}\right)^2}{1 + \left(\frac{C^{R}_{sat}}{2C^{A}_{sat}}\right)^2} \qquad (4)$$

Calculated by eq. (4) the value $ee_{eu} = 0.999$. This means that for the chiral amino acid **1** the eutectic composition is virtually indistinguishable from the composition of the enantiopure compound. Accordingly, 4-benzoylamino-3-hydroxybutyric acid **1** can be classified as a pronounced "anticonglomerate", i.e. a substance that is capable of strong enantiomeric enrichment of the predominant chiral component in solution, even in the case where the enantiomeric excess of the entire sample, distributed between the solution and the solid phase, turns out to be very small. It is possible that this behavior of substances present in the prebiotic brines is directly related to the origin of homochirality of life.[29]

Experiment on the nonequilibrium crystallization. As it was just demonstrated, the equilibrium phase behavior of amino acid **1** corresponds to a simple eutectic system "normal racemic compound ↔ pure enantiomer." But it cannot be denied, however, that the principal possibility exists of formation of metastable anomalous conglomerate in far from equilibrium conditions. Bergman and Lissitzin have attributed the structure of the anomalous molecular compound to the solid phase obtained in such conditions, namely during a rapid crystallization of the highly supersaturated aqueous solution of acid **1** sample with an enantiomeric excess of about 33%.[1]

We have repeated the experiment described in this work. For which purpose 25 mg of (*R*)-**1** was dissolved in 1 ml of water; then, 50 mg of *rac*-**1** was added to the solution, and the mixture was heated until complete dissolution. Upon reaching room temperature, the vial was filled with acicular crystals, the crystal habit of which is the same as in Figure 1b. The soaked with the mother liquor (i.e. almost saturated solution of pure enantiomer) precipitate was washed on the filter with a minimum amount of ice water. After drying in air 44 mg of the acid **1** was collected; mp 174 °C, $[\alpha]_D^{20}$ = - 4 (*c* 1.0, 0.5 N aq. NaOH). The precipitate was studied by powder diffractometry.

In Figure 10 the experimentally obtained diffraction pattern for the above prepared polycrystalline sample (black curve) is compared with the experimental diffraction patterns of pure *rac*-**1** (red curve) and (*R*)-**1** (blue curve). The black and red curves are practically identical, and this gives the reason to believe that the unit cell parameters and other characteristics of the crystal packing in both samples are the same. The coincidence of the diffraction patterns, in combination with the similar crystal habits and close to one another melting points, allows identifying the crystalline component of the precipitated in the nonequilibrium conditions solid as normal racemic compound, i.e. *rac*-**1**.

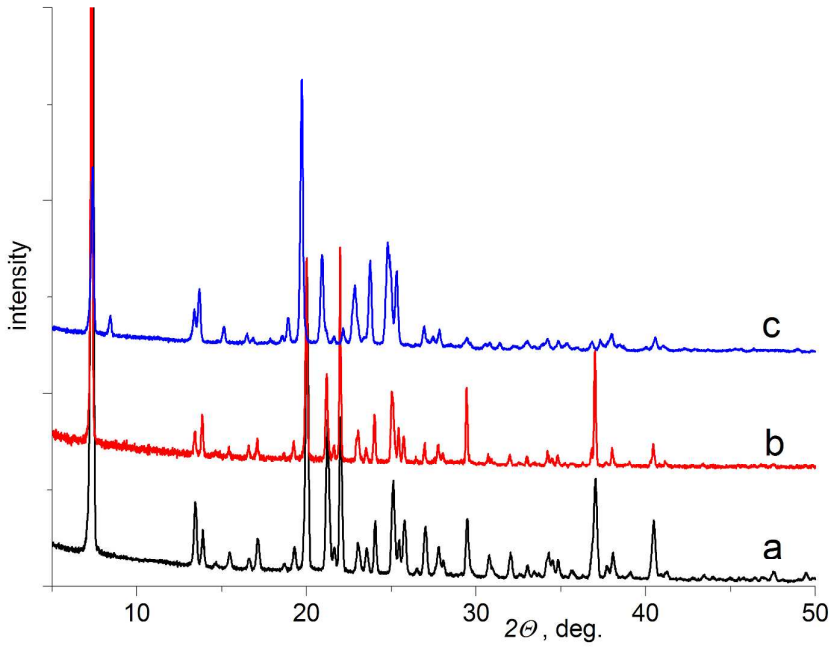

Figure 10. The experimental powder diffraction patterns for the precipitate obtained in nonequilibrium conditions (**a**, black bottom curve), for pure *rac*-**1** (**b**, red middle curve) and (*R*)-**1** (**c**, blue top curve).

The close similarity of the diffraction patterns for all the investigated samples of **1** eliminates the presence of appreciable amounts of crystalline molecular compound 2:1 among the constituents of any of the samples. In fact, the asymmetric unit of the unit cell of such a compound contains at least 3 molecules; consequently, cell volume (and hence its parameters and powder diffraction pattern) can not coincide with the corresponding characteristics of *rac*-**1** or (*R*)-**1**.

CONCLUSIONS

Based on the combined experimental studies by IR spectroscopy, single-crystal X-ray analysis, PXRD analysis, and quantitative solubility studies, we established that 4-benzoylamino-3-hydroxybutyric acid **1**, which was previously assigned as one of the first examples of "anomalous racemates", actually forms a crystalline phase of the *normal racemic compound* of composition 1:1, both in equilibrium and nonequilibrium conditions. The unit cell parameters and the crystal packing features for the racemic (heterochiral) and enantiopure (homochiral) samples of **1** are very similar to each other.

This becomes possible because *homo*-**1** sample is crystallized with two independent molecules in the asymmetric unit of the unit cell. While the conformation of one of the independent molecules in the homochiral crystal coincides with the conformation of the same enantiomer in the crystals of racemate, the conformation of the other symmetry independent molecule is more similar to the conformation of opposite enantiomer. During the formation of *homo*-**1** supramolecular crystal architecture, this second molecule mimics the antipode which is really absent in the crystals.

One might have expected that, with all the proximity of the crystallographic characteristics, the situation «quid pro quo» will lead to a significant destabilization of the crystal packing of *homo*-**1** compared with the packing of *rac*-**1**. Indeed, the solubility of *homo*-**1** is 25 times better than the solubility of *rac*-**1**, and the enantiomeric composition of the compound **1** eutectic, ee_{eu} = 0.999, is virtually indistinguishable from the composition of enantiopure substance. Based on this criterion, 4-benzoylamino-3-hydroxybutyric acid **1** behaves as a pronounced "anticonglomerate", i.e. as a substance that is capable of strong enantiomeric enrichment of the predominant chiral component in solution, even in the case where the enantiomeric excess of the entire sample, distributed between the solution and the solid phase, turns out to be very small.

ASSOCIATED CONTENT

Supporting Information

Synthetic procedures and crystallographic information files. This information is available free of charge via the Internet at http://pubs.acs.org/.

AUTHOR INFORMATION

Corresponding Author

*Phone/fax: +7 843 2727393/ +7 843 2731872; E-mail: baa@iopc.ru

Notes

The authors declare no competing financial interest.

Author Contributions

The manuscript was written through contributions of all authors. All authors have given approval to the final version of the manuscript.

ACKNOWLEDGMENT

The authors thank the Russian Fund of Basic Research for financial support (Grant No. 13-03-00174). We also wish to thank Dr. R.N. Khaybullin for valuable technical assistance.

REFERENCES

(1) Bergman, M.; Lissitzin, M. *Ber. Dtsch. Chem. Ges*. **1930**, *63*, 310–313.

(2) Jacques, J.; Collet, A.; Wilen, S. H. *Enantiomers, Racemates and Resolutions*; Krieger Publishing Company: Malabar, FL, 1994.

(3) Bredikhin, A. A.; Bredikhina, Z. A.; Zakharychev, D. V. *Mendeleev Commun*. **2012**, *22*, 171–180.

(4) Kostyanovsky, R. G.; Lyssenko, K. A.; Lenev, D. A.; Bronzova, I. A. *Tetrahedron: Asymmetry* **2002**, *13*, 2697–2701.

(5) Tabora, J. E.; Corry, J.; Osifchin, R.; Lepore, J. V.; Davidson, O. A.; Thien, M. P. *Fluid Phase Equilib.* **2007**, *258*, 140–147.

(6) Bredikhin, A. A.; Bredikhina, Z. A.; Novikova, V. G.; Pashagin, A. V.; Zakharychev, D. V.; Gubaidullin, A. T. *Chirality* **2008**, *20*, 1092–1103.

(7) Flack, H. D. *Helv. Chim. Acta* **2003**, *86*, 905–921.

(8) Dryzun, C.; Avnir, D. *Chem. Commun*. **2012**, *48*, 5874–5876.

(9) Gubaidullin, A. T.; Samigullina, A. I.; Bredikhina, Z. A.; Bredikhin, A. A. *CrystEngComm* **2014**, *16*, 6716-6729.

(10) Bishop, R.; Scudder, M. L. *Cryst. Growth Des*. **2009**, *9*, 2890–2894.

(11) Fábián, L.; Brock, C.P. *Acta Crystallogr*. **2010**, *B66*, 94-103.

(12) Kaneko, T.; Yoshida, R. *Bull. Chem. Soc. Jap*. **1962**, *35*, 1153-1154.

(13) Bergmann, M.; Brand, E., Weinmann, F. *Hoppe-Seylers Z. Physiol. Chem.* **1923**, *131*, 1–17.

(14) Sheldrick, G. M. *SADABS, Program for Empirical X-ray Absorption Correction*; Bruker-Nonius: Delft, 2004.

(15) Sheldrick, G. M. *SHELXTL, Structure Determination Software Suite*, v.6.1, Bruker AXS, Madison: Wisconsin, USA, 2000.

(16) Farrugia, L. J. *J. Appl. Crystalogr.* **1999**, *32*, 837–838.

(17) *APEX2 (Version 2.1), SAINTPlus. Data Reduction and Correction Program (Version 7.31A), Bruker Advanced X-ray Solutions*; BrukerAXS Inc.: Madison, WI, 2006.

(18) Macrae, C. F.; Edgington, P. R.; McCabe, P.; Pidcock, E.; Shields, G. P.; Taylor, R.; Towler, M.; van de Streek, J. *J. Appl. Crystallogr.* **2006**, *39*, 453–457.

(19) Spek, A. L. *J. Appl. Crystallogr.* **2003**, *36*, 7–13.

(20) Mazzetti, F.; Lemmon, R. M. *J. Org. Chem*. **1957**, *22*, 228–229.

(21) Davis, F. A.; Reddy, G. V.; Chen, B.-Ch.; Kumar, A.; Haque, M. S. *J. Org. Chem*. **1995**, *60*, 6148–6153.

(22) Bredikhin, A. A.; Bredikhina, Z. A.; Akhatova, F. S.; Zakharychev, D. V.; Polyakova, E. V. *Tetrahedron: Asymmetry* **2009**, *20*, 2130–2136.

(23) Bredikhin, A. A.; Zakharychev, D. V.; Fayzullin, R. R.; Antonovich, O. A.; Pashagin A. V.; Bredikhina, Z. A. *Tetrahedron: Asymmetry* **2013**, *24*, 807–816.

(24) Anderson, K. M.; Afarinkia, K.; Yu, H.-W.; Goeta, A. E.; Steed, J. W. *Crystal Growth & Design* **2006**, *6*, 2109-2113.

(25) Grant, D. J. W.; Takeru, H. *Solubility Behavior of Organic Compounds*; Wiley-Interscience, 1990; 656 pp.

(26) Gu, Ch.-H.; Grant, D. J. W. In *Chiral Analysis*; Bush, K.W. and Bush, M.A., Eds.; Elsevier Science B.V.: Amsterdam, The Netherlands, 2006; Chapter 3, pp 47–78.

(27) Bredikhin, A. A.; Zakharychev, D. V.; Fayzullin, R. R.; Antonovich, O. A.; Pashagin, A. V.; Bredikhina, Z. A. *Tetrahedron: Asymmetry* **2013**, *24*, 807–816.

(28) Klussmann, M.; White, A. J. P.; Armstrong, A.; Blackmond, D. G. *Angew. Chem. Int. Ed*. **2006**, *45*, 7985–7989.

(29) Hein, J. E.; Blackmond, D. G. *Acc. Chem. Res*. **2012**, *45*, 2045-2054.

For Table of Contents Use Only

4-Benzoylamino-3-hydroxybutyric acid – historically first "anomalous racemate": reinvestigation

Alexander A. Bredikhin, Zemfira A. Bredikhina, Dmitry V. Zakharychev, Aida I. Samigullina and Aidar T. Gubaidullin

The chiral 4-benzoylamino-3-hydroxybutyric acid (**1**) was earlier recognized as the first "anomalous racemate", i.e. addition compound formed of unequal numbers of different enantiomers. Based on IR, X-ray diffraction and solubility data we found that this substance forms normal racemic compound in the solid state. At the same time it belongs to another interesting and rare group, namely "anticonglomerates".

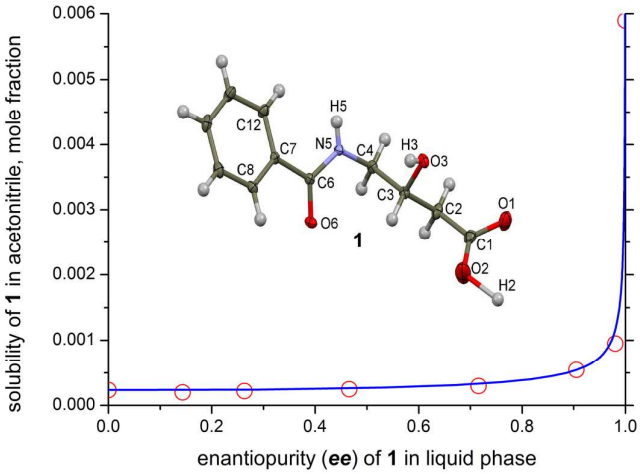

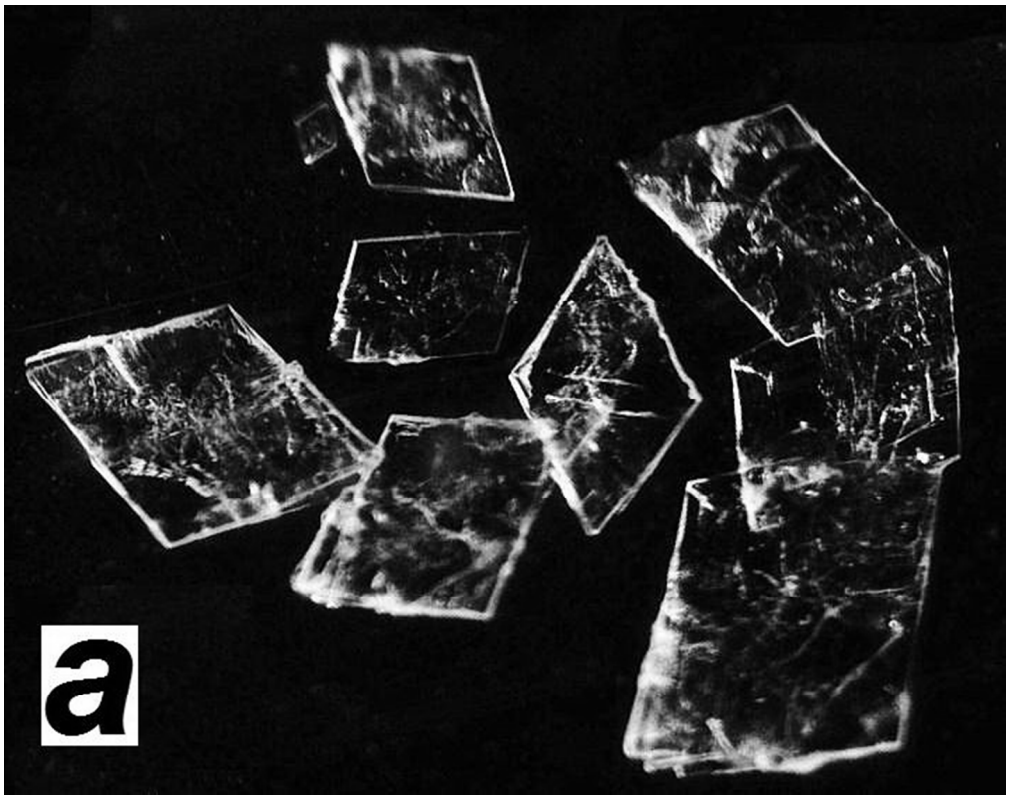

Figure 1. Microscopic pictures of the racemic and homochiral samples of compound 1. (a) Thin prisms of rac-1.1 from organic solvent; (b) needle-like crystals of rac-1.2 from water; plates of (R)-1 both from organic medium (c) and water (d).
60x47mm (300 x 300 DPI)

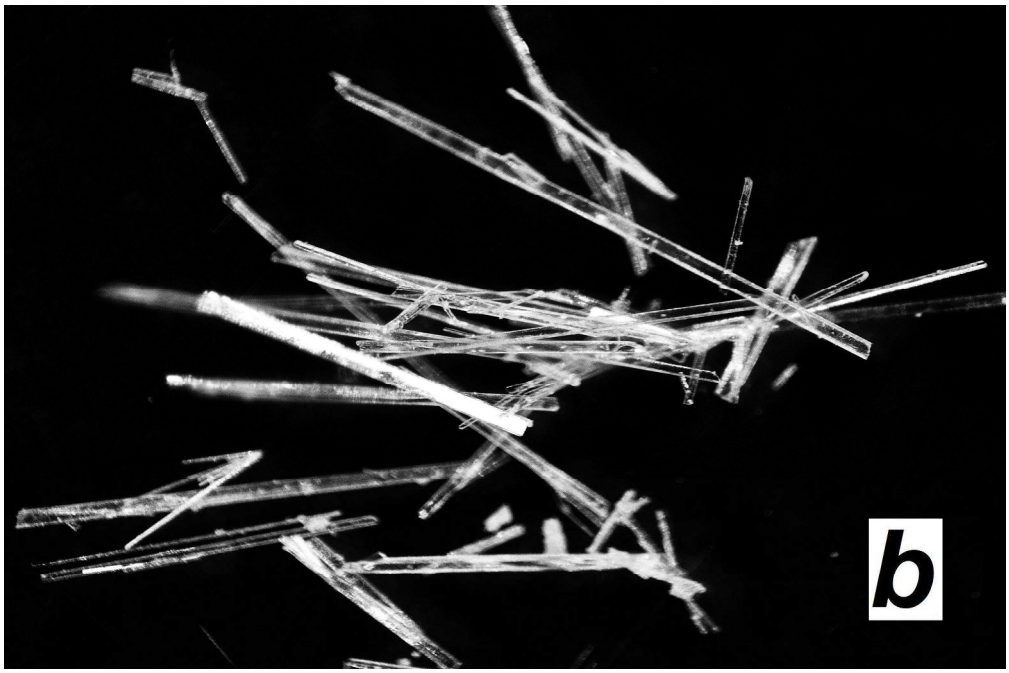

Figure 1. Microscopic pictures of the racemic and homochiral samples of compound 1. (a) Thin prisms of rac-1.1 from organic solvent; (b) needle-like crystals of rac-1.2 from water; plates of (R)-1 both from organic medium (c) and water (d).
650x431mm (96 x 96 DPI)

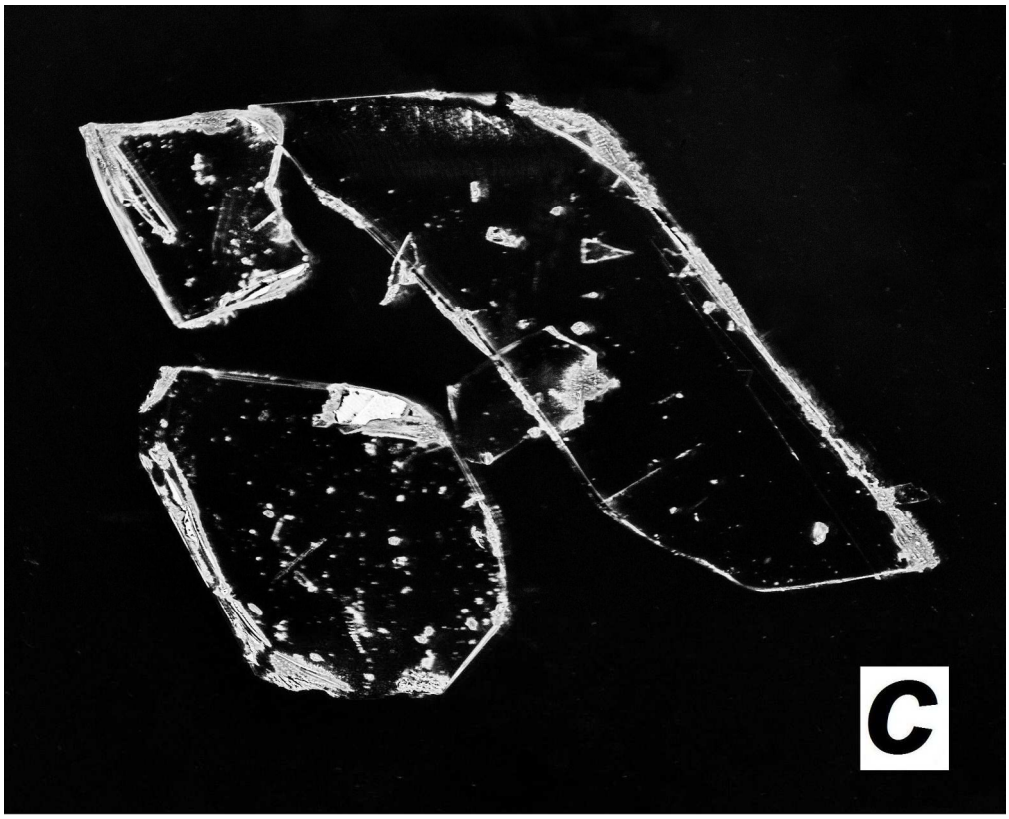

Figure 1. Microscopic pictures of the racemic and homochiral samples of compound 1. (a) Thin prisms of rac-1.1 from organic solvent; (b) needle-like crystals of rac-1.2 from water; plates of (R)-1 both from organic medium (c) and water (d).
685x553mm (72 x 72 DPI)

Figure 1. Microscopic pictures of the racemic and homochiral samples of compound 1. (a) Thin prisms of rac-1.1 from organic solvent; (b) needle-like crystals of rac-1.2 from water; plates of (R)-1 both from organic medium (c) and water (d).
101x84mm (300 x 300 DPI)

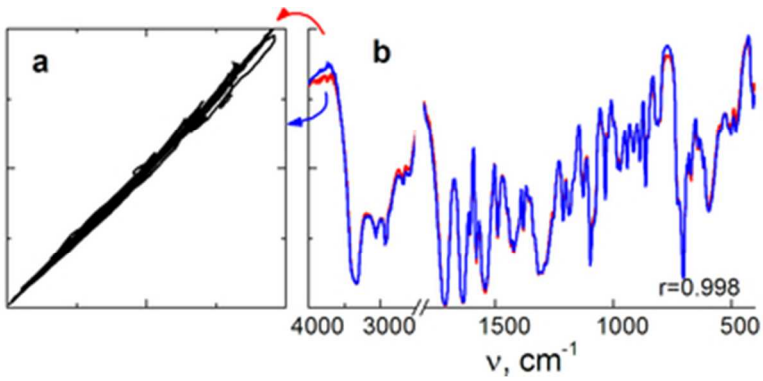

Figure 2. Correlation trajectories (a,c,e) for IR spectra in KBr pellets (b,d,f) of the pair of crystals: (R)-1 from water (red curve) against (R)-1 from ethyl acetate (blue curve) (a,b); rac-1 from water (red curve) against rac-1 from methanol/ether (blue curve) (c,d); rac-1 from methanol/ether (red curve) against (R)-1 from ethyl acetate (blue curve) (e,f).
33x15mm (300 x 300 DPI)

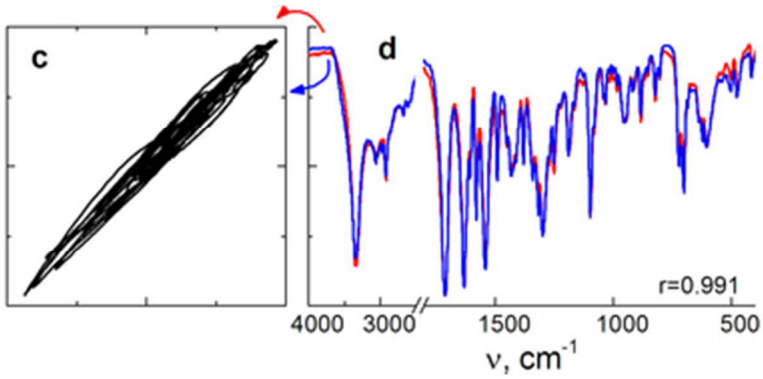

Figure 2. Correlation trajectories (a,c,e) for IR spectra in KBr pellets (b,d,f) of the pair of crystals: (R)-1 from water (red curve) against (R)-1 from ethyl acetate (blue curve) (a,b); rac-1 from water (red curve) against rac-1 from methanol/ether (blue curve) (c,d); rac-1 from methanol/ether (red curve) against (R)-1 from ethyl acetate (blue curve) (e,f).
33x15mm (300 x 300 DPI)

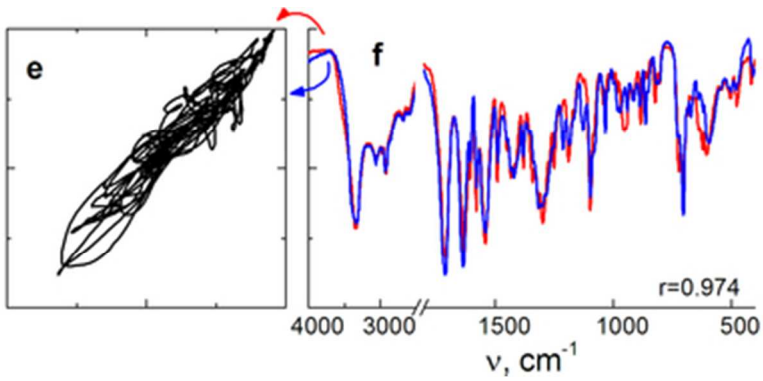

Figure 2. Correlation trajectories (a,c,e) for IR spectra in KBr pellets (b,d,f) of the pair of crystals: (R)-1 from water (red curve) against (R)-1 from ethyl acetate (blue curve) (a,b); rac-1 from water (red curve) against rac-1 from methanol/ether (blue curve) (c,d); rac-1 from methanol/ether (red curve) against (R)-1 from ethyl acetate (blue curve) (e,f).
33x15mm (300 x 300 DPI)

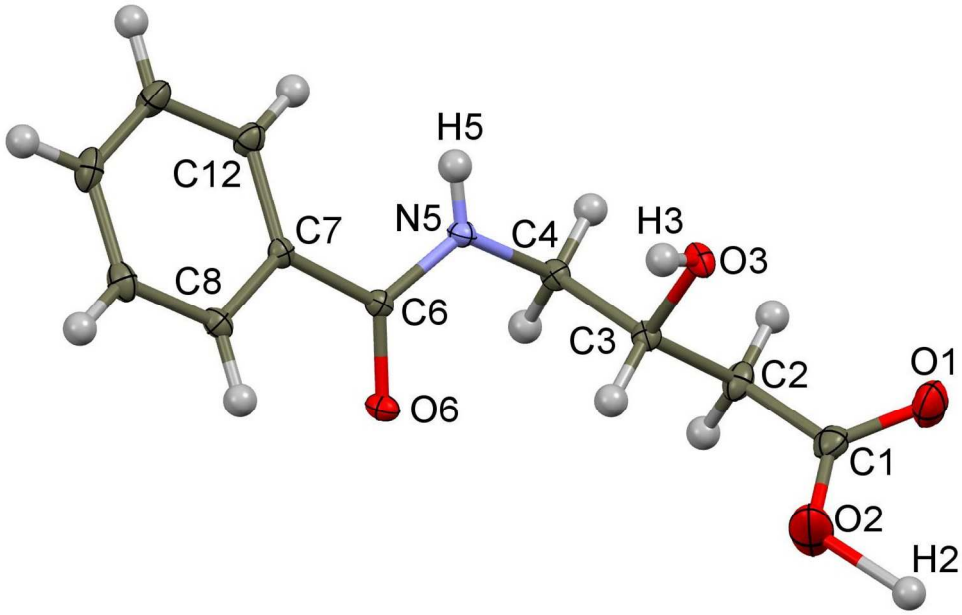

Figure 3. ORTEP plot of the molecule in the crystals of rac-1.1 and the partial numbering scheme adopted for the molecules 1 in the present work. Displacement ellipsoids are drawn at the 50% probability level, hydrogen atoms are represented as fixed-size spheres.
551x346mm (72 x 72 DPI)

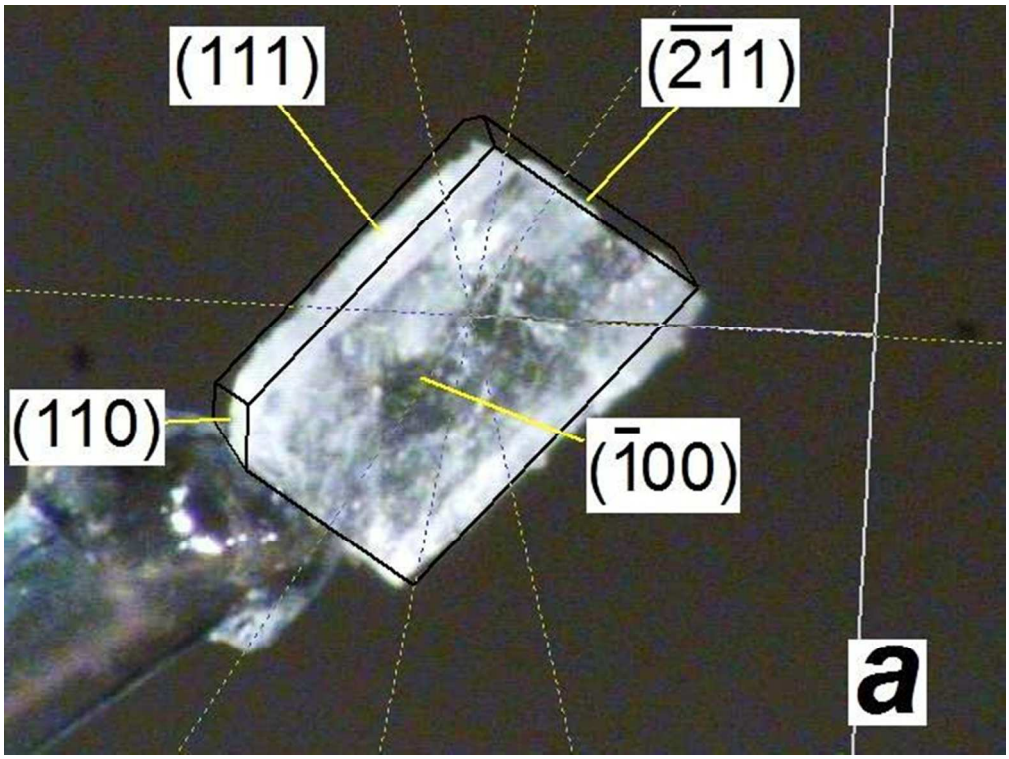

Figure 4. Miller indices of crystal faces of the rac-1.1 (a), rac-1.2 (b), and (R)-1 (c) crystals.
225x168mm (72 x 72 DPI)

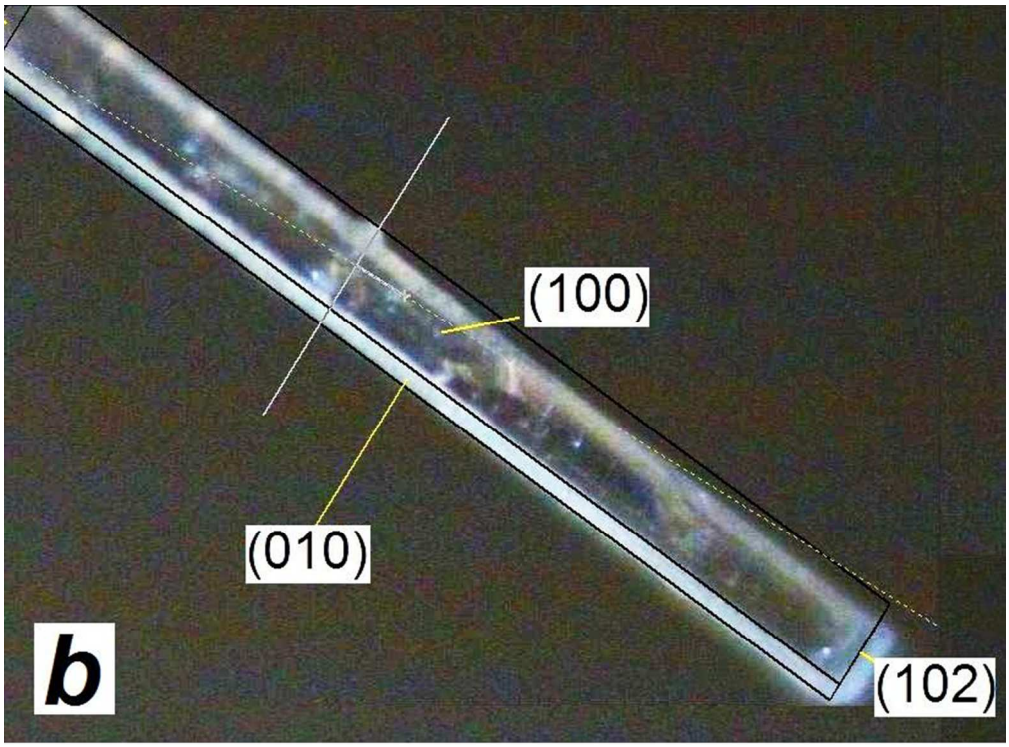

Figure 4. Miller indices of crystal faces of the rac-1.1 (a), rac-1.2 (b), and (R)-1 (c) crystals.
288x213mm (72 x 72 DPI)

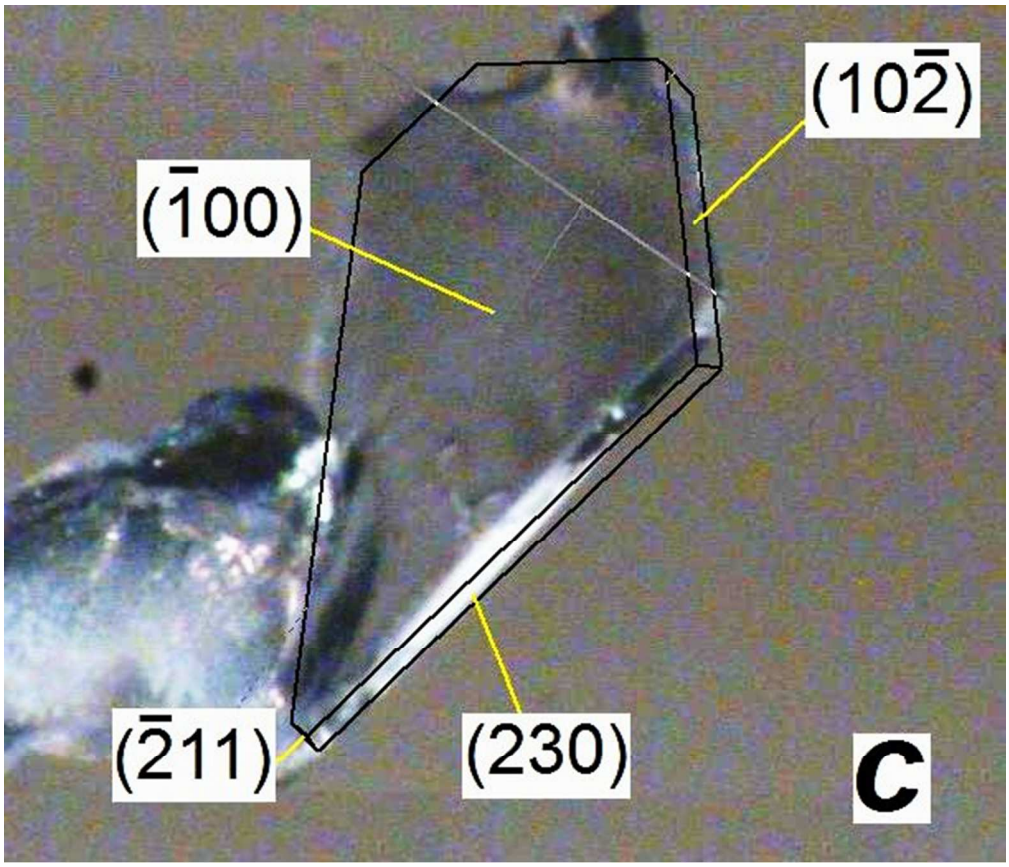

Figure 4. Miller indices of crystal faces of the rac-1.1 (a), rac-1.2 (b), and (R)-1 (c) crystals.
214x183mm (72 x 72 DPI)

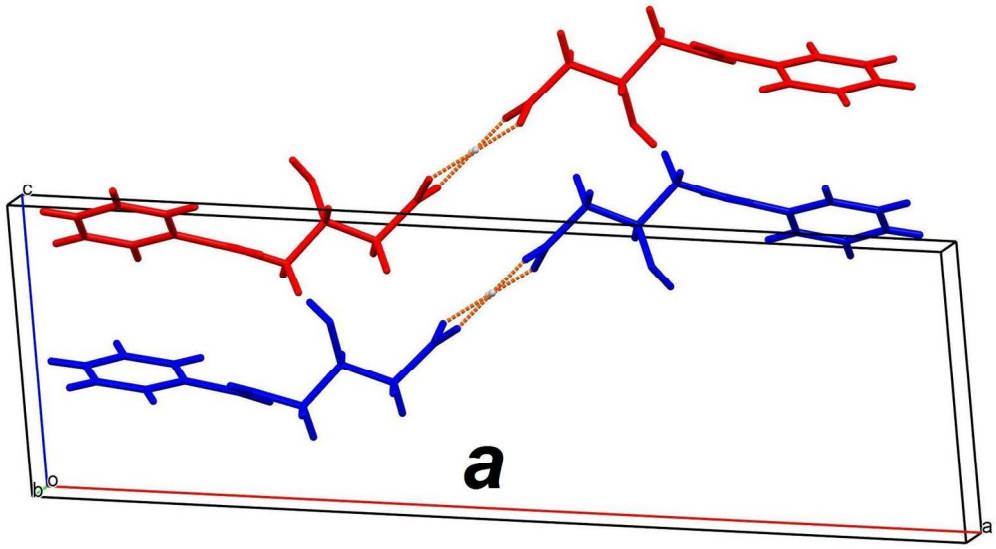

Figure 5. Supramolecular crystal structure of rac-1. (a) Zero-dimensional enantiomeric "fork" dimers; view along the 0b axis. Hereinafter dotted lines denote the intermolecular hydrogen bonds (IMHB); (R)-enantiomers colored in red, (S)-enantiomers – in blue. (b) The 1D column of "fork" dimers joined by IMHB O–H···O=C (labeled green); view along the 0b axis. (c) The same column; view along the 0c axis. (d) Merging of the one-dimensional columns into a three-dimensional supramolecular structure through IMHB NH···OH (marked in red); view along the 0c axis.
635x352mm (72 x 72 DPI)

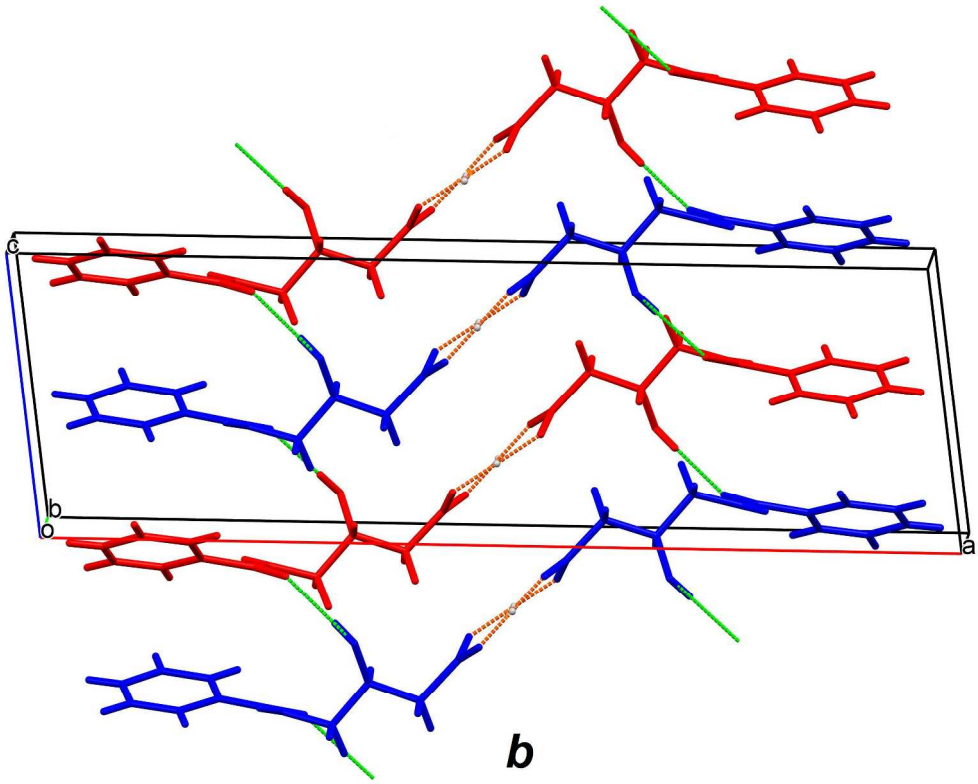

Figure 5. Supramolecular crystal structure of rac-1. (a) Zero-dimensional enantiomeric "fork" dimers; view along the 0b axis. Hereinafter dotted lines denote the intermolecular hydrogen bonds (IMHB); (R)-enantiomers colored in red, (S)-enantiomers – in blue. (b) The 1D column of "fork" dimers joined by IMHB O–H···O=C (labeled green); view along the 0b axis. (c) The same column; view along the 0c axis. (d) Merging of the one-dimensional columns into a three-dimensional supramolecular structure through IMHB NH···OH (marked in red); view along the 0c axis.
808x641mm (96 x 96 DPI)

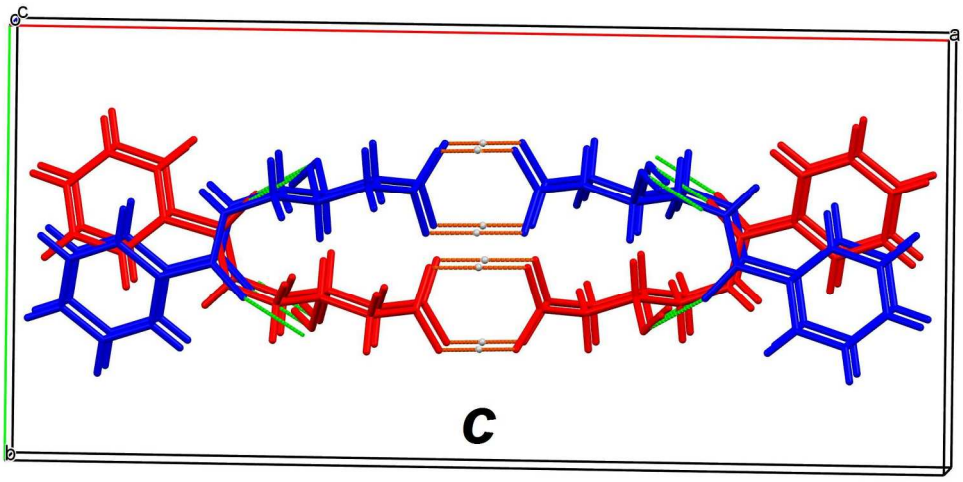

Figure 5. Supramolecular crystal structure of rac-1. (a) Zero-dimensional enantiomeric "fork" dimers; view along the 0b axis. Hereinafter dotted lines denote the intermolecular hydrogen bonds (IMHB); (R)-enantiomers colored in red, (S)-enantiomers – in blue. (b) The 1D column of "fork" dimers joined by IMHB O–H···O=C (labeled green); view along the 0b axis. (c) The same column; view along the 0c axis. (d) Merging of the one-dimensional columns into a three-dimensional supramolecular structure through IMHB NH···OH (marked in red); view along the 0c axis.
587x295mm (96 x 96 DPI)

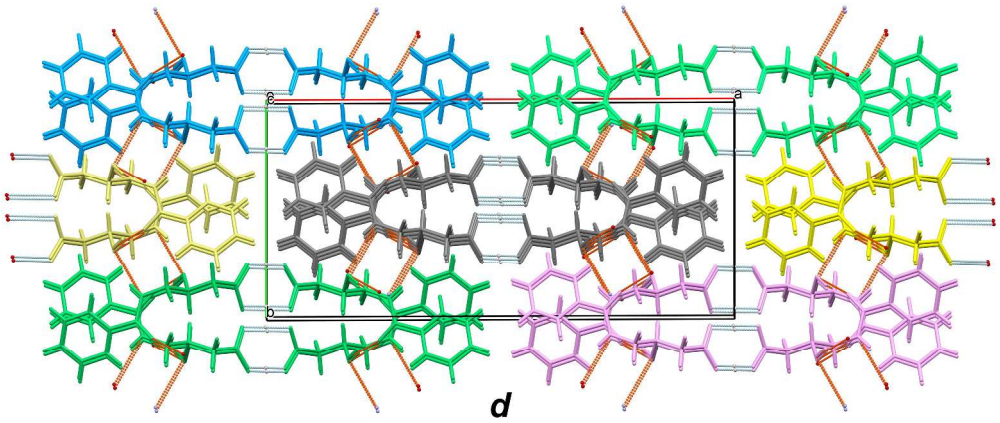

Figure 5. Supramolecular crystal structure of rac-1. (a) Zero-dimensional enantiomeric "fork" dimers; view along the 0b axis. Hereinafter dotted lines denote the intermolecular hydrogen bonds (IMHB); (R)-enantiomers colored in red, (S)-enantiomers – in blue. (b) The 1D column of "fork" dimers joined by IMHB O–H···O=C (labeled green); view along the 0b axis. (c) The same column; view along the 0c axis. (d) Merging of the one-dimensional columns into a three-dimensional supramolecular structure through IMHB NH···OH (marked in red); view along the 0c axis.
1369x591mm (96 x 96 DPI)

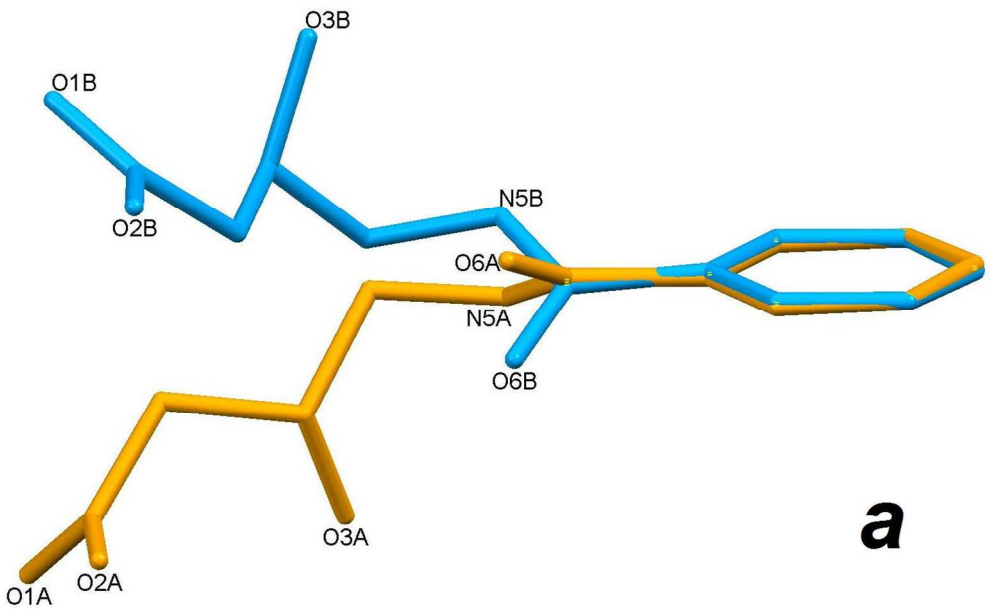

Figure 6. Conditional superposition of the molecules existing in the amino acid 1 crystals. (a) Two independent molecules, A (orange) and B (light blue), in the crystal of (R)-1. (b) Molecule A (orange) in (R)-1 crystal and molecule of R-enantiomer (red) in the crystals of rac-1. (c) Molecule B (light blue) in (R)-1 crystal and molecule of (S)-enantiomer (blue) in the crystals of rac-1.
389x239mm (96 x 96 DPI)

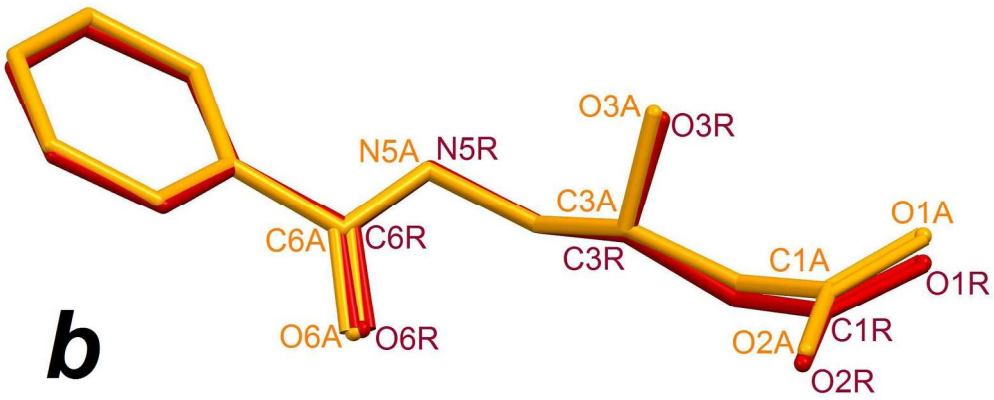

Figure 6. Conditional superposition of the molecules existing in the amino acid 1 crystals. (a) Two independent molecules, A (orange) and B (light blue), in the crystal of (R)-1. (b) Molecule A (orange) in (R)-1 crystal and molecule of R-enantiomer (red) in the crystals of rac-1. (c) Molecule B (light blue) in (R)-1 crystal and molecule of (S)-enantiomer (blue) in the crystals of rac-1.
541x218mm (96 x 96 DPI)

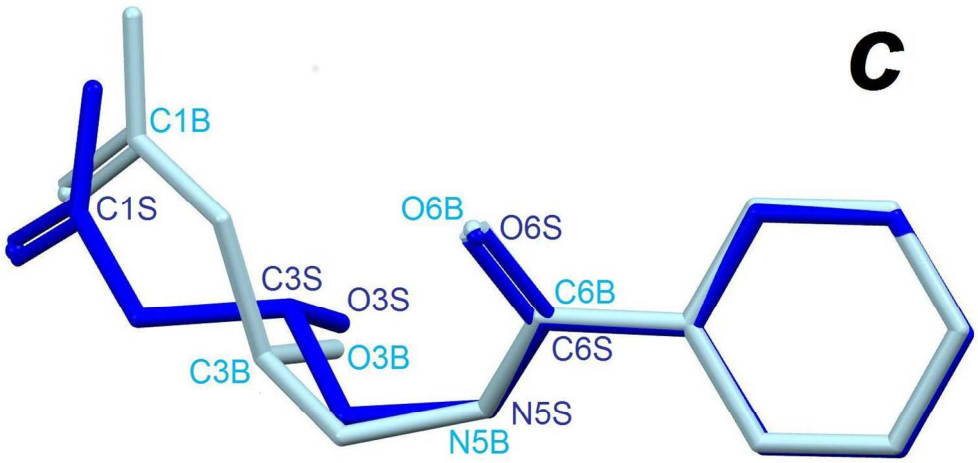

Figure 6. Conditional superposition of the molecules existing in the amino acid 1 crystals. (a) Two independent molecules, A (orange) and B (light blue), in the crystal of (R)-1. (b) Molecule A (orange) in (R)-1 crystal and molecule of R-enantiomer (red) in the crystals of rac-1. (c) Molecule B (light blue) in (R)-1 crystal and molecule of (S)-enantiomer (blue) in the crystals of rac-1.
397x208mm (96 x 96 DPI)

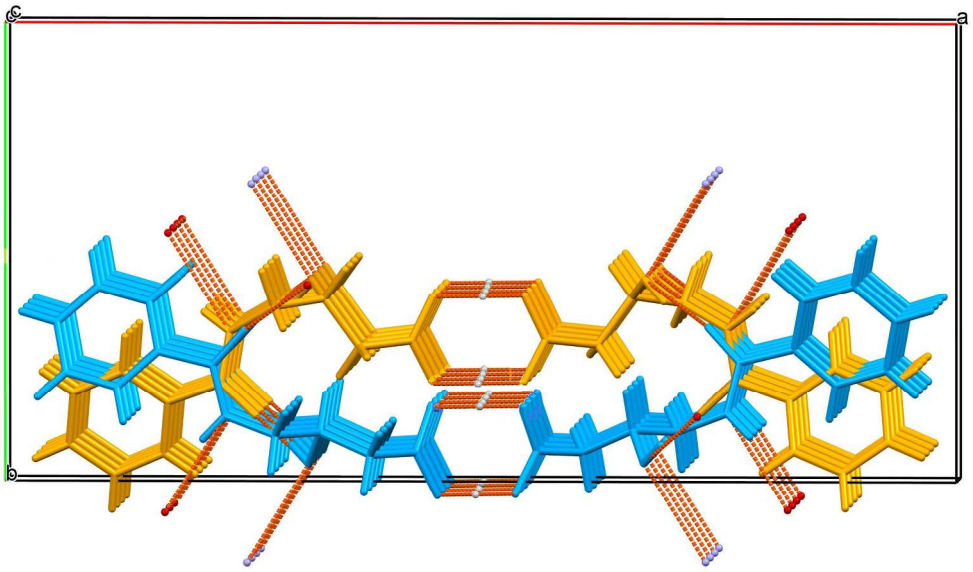

Figure 7. 1D column formed by independent molecules A and B in the crystals of (R)-1. View along 0c axis.
681x403mm (96 x 96 DPI)

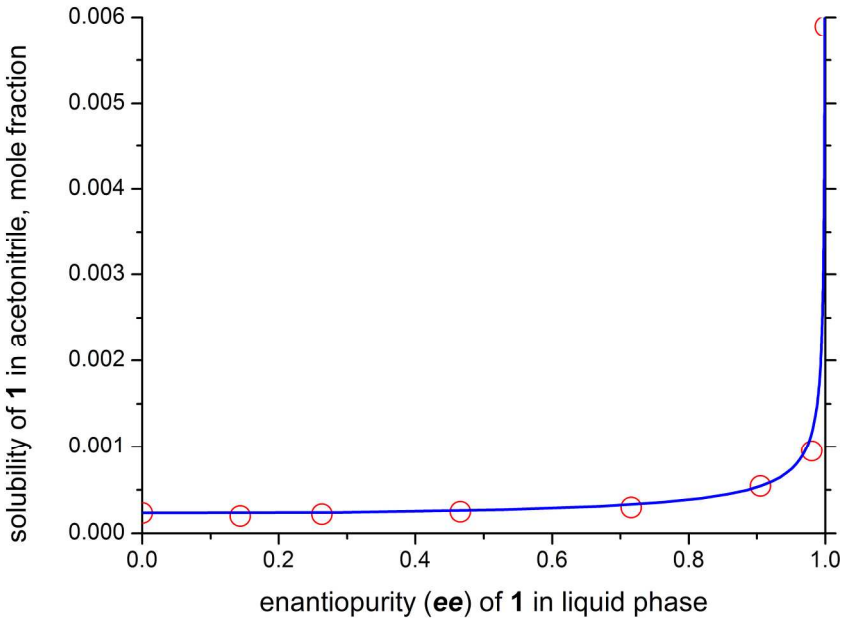

Figure 8. The dependence between the amino acid 1 solubility in acetonitrile and the enantiomeric excess of 1 in solution. Red circles - the experimental solubility values, blue curve - the values calculated under the assumption that the single racemic compound is formed in the system.
203x146mm (300 x 300 DPI)

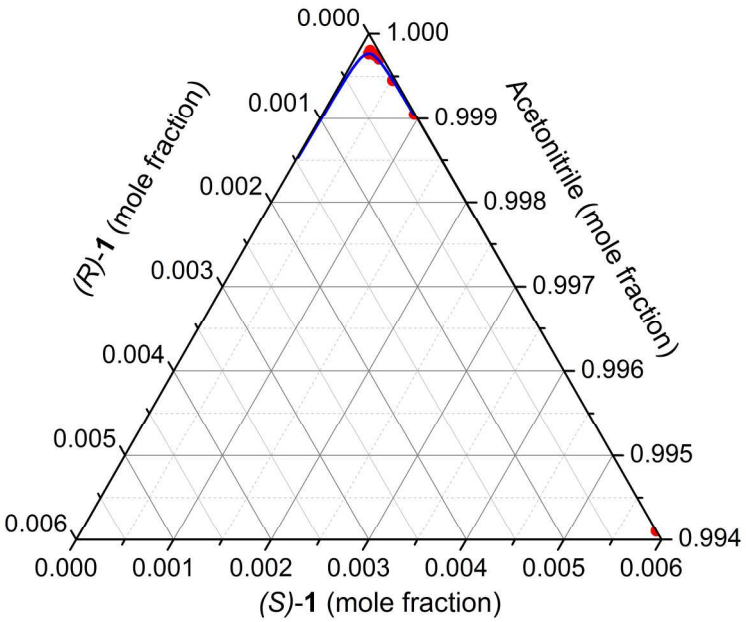

Figure 9. Ternary phase solubility diagram (fragment) in the system CH3CN/(R)-1/(S)-1. Red circles - the experimental values of the equilibrium composition of the liquid phase.
203x146mm (300 x 300 DPI)

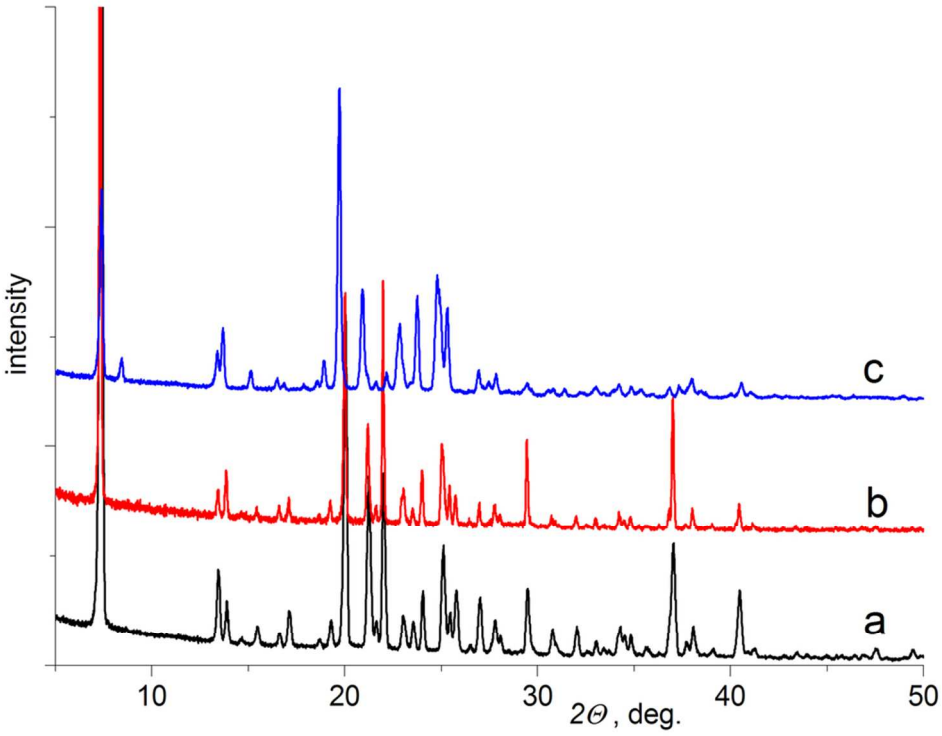

Figure 10. The experimental powder diffraction patterns for the precipitate obtained in nonequilibrium conditions (a, black bottom curve), for pure rac-1 (b, red middle curve) and (R)-1 (c, blue top curve).
89x67mm (300 x 300 DPI)